Journal of Applied Analysis and Computation
Volume 14, Number 3, June 2024, 1269–1301
Website:http://www.jaac-online.com
DOI:10.11948/20230087

STABILIZED PRIMAL AND DUAL HYBRID MIXED DGFEM FOR DARCY FLOW*

Iury Igreja[1,†]

Abstract This work presents and analyzes two stabilized mixed hybrid Discontinuous Galerkin Finite Element Methods (DGFEM) for Darcy flows. The difference between the methodologies lies in the choice of Lagrange multipliers that aim to weakly enforce continuity on the edge/face of the elements. Thus, we study methods with multipliers associated with the normal component of the velocity field and the trace of the pressure field that naturally gives rise, respectively, to primal and dual formulations. However, despite the difference between the formulations, both methods can be associated with the same discontinuous Galerkin formulation. In this sense, the analysis of consistency, existence, uniqueness, and error estimates is similar for both methods, even when continuous interpolations are employed to approximate the Lagrange multipliers. Moreover, stability and convergence rate are improved by adding the least-squares residual forms of the governing equations. Besides, for specific edge/face stabilization parameter choices, the methods become locally conservative, allowing the use of non-conforming Raviart-Thomas spaces. Finally, to illustrate the accuracy, convergence rates, local mass conservation, computational efficiency, and flexibility of the methods, several two and three-dimensional numerical experiments are performed considering homogeneous and heterogeneous porous media.

Keywords Darcy problem, primal and dual formulation, hybrid-mixed methods, discontinuous Galerkin, stabilization.

MSC(2010) 65N12, 65N15, 65N30, 76S05.

1. Introduction

The incompressible fluid flow in the porous media has been extensively studied due to several applications in petroleum engineering, hydrogeology, biofluid dynamics, and filtration, among others. This problem is modeled by the classical Darcy system, which consists of the mass conservation equation plus Darcy's law, which relates the average velocity of the fluid in a porous medium with the gradient of a potential field through the hydraulic conductivity tensor. Several numerical methods have been employed in the last decades to approximate this system of partial

†the corresponding author.
[1]Department of Computer Science and Graduate Program on Computational Modeling, Federal University of Juiz de Fora, Rua José Lourenço Kelmer – São Pedro – Juiz de Fora, 36036-900, Minas Gerais, Brazil
*This study is supported by CAPES (Brazil grant 88881.708850/2022-01), CNPq (Brazil grants 405366/2021-3 and 305353/2022-5) and FAPEMIG (Brazil grant APQ-00517-21).
Email: iuryigreja@ice.ufjf.br(I. Igreja)

differential equations. In particular, mixed finite element methods have been developed. However, the classical finite element approximations for these problems present limitations due to the necessity to satisfy an inf-sup compatibility condition between the space of approximations [9, 11, 12]. To overcome this limitation, [29] and [13] developed combinations of the approximation spaces based on the imposition the continuity of the normal component of the velocity field in combination with specific discontinuous interpolations for the pressure. More recently, examples of stable spaces for this problem were proposed by [5] and [2].

On another front, where this work is focused, the class of finite element methods is stabilized by adding least-squares residual terms of the model problem to preserve the consistency and symmetry of the formulation. This technique is known in the literature by Galerkin Least-Square (GLS) methods [10, 14, 19, 26] that, unlike the classical formulations in which the stability is limited to specific finite element spaces, are unconditionally stable and add more flexibility in the finite element approximations construction as, for example, the same polynomial order approximations for the velocity and pressure fields. Thus, stabilized methods add terms to classical variational formulations, making the discrete approximations, which would otherwise be unstable, stable, and convergent.

Discontinuous Galerkin (DG) methods have also been proposed to solve the Darcy problem due to their flexibility in choosing approximation spaces and implementing h and p adaptivity strategies and parallelization [15, 16, 22]. More recently, hybridized versions of DG methods have been introduced that preserve the properties of DG methods but with improved stability and reduced implementation complexity and computational cost [8, 25, 31]. The hybrid formulations allow, from appropriate choices, the elimination of the local problems at each element level in favor of the Lagrange multiplier [24]. Thus, the system involves only global degrees of freedom associated with the multiplier. Some references that apply this technique to solve Darcy's Problem can be found in the works of [17, 18, 25, 28].

In this context, we study two stabilized hybrid approaches based on the Darcy problem's primal and dual formulations. In both formulations, we add least-squares residuals of Darcy's law and the mass balance equation, which leads to flexibility in the choice of finite element spaces and optimal convergence properties in an energy norm equivalent to a mesh dependent $H(\mathrm{div}) \times H^1$-norm [19, 22, 25, 26]. In this context, we propose the Stabilized Primal Hybrid Mixed (SPHM) method, which, unlike the method presented and analyzed in [25], whose Lagrange multiplier is a vector associated with the velocity field, the proposed method only imposes the continuity of the normal velocity component at the interfaces of the elements. The scalar Lagrange multiplier associated with the normal component of the velocity field makes possible the natural treatment of the heterogeneities generated by the permeability of the porous matrix, the use of non-conforming Raviart-Thomas spaces, and also significantly reduces the size of the global problem. On the other hand, the Stabilized Dual Hybrid Mixed (SDHM) method employs Lagrange multipliers related to the pressure field. The SDHM method was first introduced in [28] considering discontinuous interpolations for the Lagrange multiplier. However, the contribution here is to perform the analysis and numerical studies adopting continuous interpolations for the Lagrange multiplier. Another contribution of this work is to connect the hybrid formulations to a DG method by eliminating the Lagrange multiplier to employ the same arguments to prove the consistency, stability, continuity, and convergence of both hybrid techniques. Moreover, both methods

become locally conservative from appropriate choices for the edge/face stabilization coefficient, allowing the use of non-conforming Raviart-Thomas spaces [6, 29].

To validate, establish accuracy, and confirm the convergence rates of the proposed SPHM method and the SDHM method with continuous interpolations for the Lagrange multiplier, we conducted an extensive numerical investigation in two- and three-dimensions on homogeneous and heterogeneous porous media. In this context, these methods are compared through h- and p-convergence studies. Furthermore, an analysis of local mass conservation based on the variation of the penalty parameter is presented, a study is carried out regarding the computational cost of assembling and solving these methods, and Jacobi and Symmetric Successive Over-Relaxation (SSOR) preconditioners are tested to compare their performances.

This paper is organized as follows. In Section 2, the Darcy problem, notations, and definitions are introduced. In Section 3, Primal and Dual hybrid mixed methods and their connection with the same DG method are presented. The consistency, stability, continuity, and error estimates of these methods are proved in Section 4. Section 5 presents the computational strategy to solve these methods. In Section 6, we validate and compare the formulations through convergence studies considering homogeneous and heterogeneous porous media. Finally, Sections 7 and 8 present the discussions and concluding remarks of this work.

2. Preliminares

This section presents the model problem and some definitions and notations commonly adopted to construct variational formulations in broken function spaces associated with DG and hybrid mixed methods.

2.1. Model problem

The flow of a Newtonian and incompressible fluid through a rigid porous medium is governed by a system of partial differential equations formed by the mass conservation combined with Darcy's law, which relates to the flow velocity average in the pores with a potential gradient. Therefore, in a bounded domain $\Omega \subset \mathbb{R}^d$, $d = 2$ or 3 with Lipschitz boundary $\Gamma = \partial\Omega$, we present the Darcy system as follows:

Given the function f, find the fluid velocity $\mathbf{u} : \Omega \to \mathbb{R}^d$ and the hydrostatic pressure $p : \Omega \to \mathbb{R}$, such that

$$\mathbf{u} = -\mathbf{K}\nabla p \qquad \text{in} \quad \Omega, \tag{2.1}$$

$$\operatorname{div} \mathbf{u} = f \qquad \text{in} \quad \Omega, \tag{2.2}$$

where ∇ and div denotes the gradient and divergent operators, respectively, and $\mathbf{K}$ the hydraulic conductivity tensor. This problem can be supplemented by Neumann boundary conditions

$$\mathbf{u} \cdot \mathbf{n} = 0 \qquad \text{on} \quad \Gamma, \tag{2.3}$$

where the source f must satisfy the compatibility condition

$$\int_\Omega f \, d\mathbf{x} = 0,$$

or Dirichlet boundary conditions

$$p = 0 \qquad \text{on} \quad \Gamma. \tag{2.4}$$

2.2. Notations and definitions

Let $H^m(\Omega)$ denote the usual Sobolev space equipped with a norm $\|\cdot\|_{m,\Omega} = \|\cdot\|_m$ and semi-norm $|\cdot|_{m,\Omega} = |\cdot|_m$, with $m \geq 0$. For $m = 0$, we present $L^2(\Omega) = H^0(\Omega)$ as the space of square-integrable functions and $H_0^1(\Omega)$ the subspace of functions in $H^1(\Omega)$ with zero trace on $\partial\Omega$. In addition, we set

$$L_0^2(\Omega) = \{\phi \in L^2(\Omega) : \int_\Omega \phi \, d\mathbf{x} = 0\}.$$

We also define the Hilbert space associated to the divergence operator

$$H(\mathrm{div}, \Omega) = H(\mathrm{div}) = \{\mathbf{w} \in [L^2(\Omega)]^d, \, \mathrm{div}\, \mathbf{w} \in L^2(\Omega)\},$$

with norm

$$\|\mathbf{w}\|^2_{H(\mathrm{div})} = \|\mathbf{w}\|_0^2 + \|\mathrm{div}\, \mathbf{w}\|_0^2.$$

Let $\mathcal{T}_h$ be a regular finite element partition of the domain Ω, defined by

$$\mathcal{T}_h = \{K\} := \text{the union of all elements } K$$

and let $\mathcal{E}_h = \{e;\, e \text{ is an edge/face of } K \text{ for all } K \in \mathcal{T}_h\}$ denotes the set of all edges/faces e of all elements K, $\mathcal{E}_h^0 = \{e \in \mathcal{E}_h;\, e \text{ is an interior edge/face}\}$ is the set of interior edges/faces, and $\mathcal{E}_h^\partial = \{e \in \mathcal{E}_h; e \subset \partial\Omega\}$ is the set of edges/faces of $\mathcal{E}_h$ on the boundary of Ω. We assume that the domain Ω is polygonal and $\mathcal{T}_h$ is a regular partition of Ω. Thus, there exists $c > 0$ such that $h \leq ch_e$, where h_e is the diameter of the edge/face $e \in \partial K$ and h, the mesh parameter is the element diameter. For each element K, we associate a unit outward normal vector $\mathbf{n}_K$.

For a scalar-valued function $\phi \in L^2(\Omega)$ with $\phi|_K \in H^m(K)$ for all $K \in \mathcal{T}_h$, let $|\phi|_{m,h}$ be the usual broken H^m-type semi-norm of ϕ defined by

$$|\phi|_{m,h} = \left(\sum_{K \in \mathcal{T}_h} |\phi|^2_{m,K} \right)^{1/2} = \left(\sum_{K \in \mathcal{T}_h} \int_K |\nabla^m \phi|^2 dx \right)^{1/2}. \tag{2.5}$$

If $\mathbf{w}$ is a vector-valued or tensor-valued function, the corresponding term $\|\mathbf{w}\|_{m,h}$ is defined in a similar manner. For a vector or a tensor $\mathbf{w}$, we denote by $|\mathbf{w}|$ the quantity $(\mathbf{w} \cdot \mathbf{w})^{1/2}$ or $(\mathbf{w} : \mathbf{w})^{1/2}$, respectively.

To establish a connection between the hybrid methods with discontinuous Galerkin methods, we introduce some definitions usually applied to formulate and analyze the DG methods. Thus, given the elements $K^+, K^- \in \mathcal{T}_h$ sharing the edge/face e, we define the corresponding outward unit normal vectors $\mathbf{n}_{K^+}$ and $\mathbf{n}_{K^-}$ on e to K^+ and K^-. For a scalar function ϕ and a vector-valued function $\mathbf{w}$ that is smooth inside each element $K^\pm$, let us denote by $(\phi^\pm, \mathbf{w}^\pm)$ the traces of $(\phi, \mathbf{w})$ on e taken from within the interior of $K^\pm$, respectively. Thus, we define the following averages

$$\{\!\{\phi\}\!\} = \frac{1}{2}(\phi^+ + \phi^-); \qquad \{\!\{\mathbf{w}\}\!\} = \frac{1}{2}(\mathbf{w}^+ + \mathbf{w}^-) \qquad \text{on } e \in \mathcal{E}_h^0, \tag{2.6}$$

and analogously, we define the jumps as

$$[\![\phi]\!] = \phi^+ \mathbf{n}_{K^+} + \phi^- \mathbf{n}_{K^-}; \quad [\![\mathbf{w}]\!] = \mathbf{w}^+ \cdot \mathbf{n}_{K^+} + \mathbf{w}^- \cdot \mathbf{n}_{K^-} \quad \text{on } e \in \mathcal{E}_h^0. \tag{2.7}$$

For edges/faces on the boundary of the domain, it is usually set

$$\{\!\{\phi\}\!\} = \phi, \quad [\![\phi]\!] = \phi\, \mathbf{n}; \qquad \{\!\{\mathbf{w}\}\!\} = \mathbf{w}, \quad [\![\mathbf{w}]\!] = \mathbf{w} \cdot \mathbf{n} \quad \text{on } e \in \mathcal{E}_h^\partial \tag{2.8}$$

where $\mathbf{n}$ is the unit outward normal vector on Γ.

Based on the above definitions, we present the following identity (see [7] and [15])

$$\sum_{K \in \mathcal{T}_h} \int_{\partial K} \phi(\mathbf{w} \cdot \mathbf{n}_K) ds = \sum_{e \in \mathcal{E}_h} \int_e \{\!\{\phi\}\!\}\, [\![\mathbf{w}]\!] ds + \sum_{e \in \mathcal{E}_h^0} \int_e [\![\phi]\!] \cdot \{\!\{\mathbf{w}\}\!\}\, ds. \tag{2.9}$$

Let $\mathcal{V}_h$ and $\mathcal{Q}_h$ denote the broken function spaces on the partition of $\mathcal{T}_h$, given by

$$\mathcal{V}_h^k = \{\mathbf{w} \in [L^2(\Omega)]^d; \mathbf{w}|_K \in [\mathbb{Q}_k(K)]^d, \ \forall K \in \mathcal{T}_h\}, \tag{2.10}$$

$$\mathcal{Q}_h^l = \{\phi \in L^2(\Omega); \phi|_K \in \mathbb{Q}_l(K), \ \forall K \in \mathcal{T}_h\}, \tag{2.11}$$

where $\mathbb{Q}_j(K)$ is the product space of polynomial functions of degree at most j in each space variable associated with quadrilateral/hexahedral elements, with $j = k$ or $j = l$. Furthermore, to simplify the notation, we use throughout the text $\mathbb{Q}_k = [\mathbb{Q}_k]^d$. Also, on the edges/faces $e \in \mathcal{E}_h$, we define the Lagrange multiplier spaces

$$\mathcal{D}_h^k = \{\mu \in L^2(\mathcal{E}_h) : \mu|_e = p_k(e), \ \forall e \in \mathcal{E}_h^0, \mu|_e = 0, \ \forall e \in \mathcal{E}_h^\partial\}, \tag{2.12}$$

$$\mathcal{C}_h^k = \{\mu \in C^0(\mathcal{E}_h) : \mu|_e = p_k(e), \ \forall e \in \mathcal{E}_h^0, \mu|_e = 0, \ \forall e \in \mathcal{E}_h^\partial\}. \tag{2.13}$$

Similarly, $p_k(e)$ is the space of polynomial functions of degree at most k on an edge/face e. The space $\mathcal{D}_h^k$ consider discontinuous interpolations for the Lagrange multiplier and $\mathcal{C}_h^k$ the continuous interpolations. The set of admissible continuous and discontinuous functions is defined as

$$\mathcal{M}_h^k \in \{\mathcal{D}_h^k, \mathcal{C}_h^k\}. \tag{2.14}$$

3. Stabilized Hybrid Mixed methods

In this section, we introduce a Stabilized Primal Hybrid Mixed (SPHM) formulation for the Darcy problem and recall the Stabilized Dual Hybrid Mixed (SDHM) method adopting continuous and discontinuous interpolations for the Lagrange multipliers [28]. The SPHM method is characterized by the weak imposition of the continuity via Lagrange multipliers associated with the normal velocity component on the edges/faces of the elements. On the other hand, the SDHM method is identified by the Lagrange multipliers related to the pressure field on the edges/faces of the elements. From an appropriate choice of the interface stabilization parameter, both formulations generate the same associated DG method when we eliminate the Lagrange multipliers.

To this end, first, we define the model problem (2.1)-(2.3) posed on each element K of the mesh $\mathcal{T}_h$ as the set of local problems

$$\mathbf{A}\mathbf{u} = -\nabla p \quad \text{in} \quad K, \tag{3.1}$$

$$\operatorname{div} \mathbf{u} = f \quad \text{in} \quad K, \tag{3.2}$$

$$[\![\mathbf{u}]\!] = \mathbf{u} \cdot \mathbf{n} = 0 \quad \forall e \in \mathcal{E}_h^{\partial}, \tag{3.3}$$

with the following transmission conditions

$$[\![\mathbf{u}]\!] = 0 \quad \text{and} \quad [\![p]\!] = \mathbf{0}, \qquad \forall e \in \mathcal{E}_h^0, \tag{3.4}$$

where $\mathbf{A} = \mathbf{K}^{-1}$ denotes the hydraulic resistivity tensor and $[\![\cdot]\!]$ is the jump operator defined in (2.7). From the definition of the problem at the element level, we next introduce the stabilized hybrid mixed primal and dual formulations.

3.1. Stabilized Primal Hybrid Mixed method

Considering the equations (3.1)-(3.2) multiplied by their respective weighting functions in the spaces $[L^2(K)]^d$ and $H^1(K)$ using the integration by parts on each element $K \in \mathcal{T}_h$, leads to the following local weak form

$$\int_K \mathbf{A}\mathbf{u} \cdot \mathbf{v}\, d\mathbf{x} + \int_K \nabla p \cdot \mathbf{v}\, d\mathbf{x} = 0, \quad \forall \mathbf{v} \in [L^2(K)]^d, \tag{3.5}$$

$$\int_K \mathbf{u} \cdot \nabla q\, d\mathbf{x} - \int_{\partial K} (\mathbf{u} \cdot \mathbf{n}_K)\, q\, ds = -\int_K f\, q\, d\mathbf{x}, \quad \forall q \in H^1(K). \tag{3.6}$$

An approximation to the formulation (3.5)-(3.6) can be obtained in the spaces $\mathcal{V}_h^k$ and $\mathcal{Q}_h^l$ defined, respectively, in (2.10) and (2.11), generating the approximation for each element $K \in \mathcal{T}_h$

$$\int_K \mathbf{A}\mathbf{u}_h \cdot \mathbf{v}_h\, d\mathbf{x} + \int_K \nabla p_h \cdot \mathbf{v}_h\, d\mathbf{x} = 0, \quad \forall \mathbf{v}_h \in \mathcal{V}_h^k, \tag{3.7}$$

$$\int_K \mathbf{u}_h \cdot \nabla q_h\, d\mathbf{x} - \int_{\partial K} (\mathbf{u}_h \cdot \mathbf{n}_K)\, q_h\, ds = -\int_K f\, q_h\, d\mathbf{x}, \quad \forall q_h \in \mathcal{Q}_h^l. \tag{3.8}$$

Adding (3.7) and (3.8), choosing the multiplier associated with the normal component of the velocity field $\lambda^n = \mathbf{u} \cdot \mathbf{n}_K|_e$ on each edge/face $e \in \mathcal{E}_h$ belonging to space $\mathcal{D}_h^k$ and introducing a consistent stabilization term related to λ^n governed by the edge/face stabilization parameter β_n, defined as

$$\beta_n = Ah\beta_0, \tag{3.9}$$

we obtain

$$\begin{aligned} &\int_K \mathbf{A}\mathbf{u}_h \cdot \mathbf{v}_h\, d\mathbf{x} + \int_K \nabla p_h \cdot \mathbf{v}_h\, d\mathbf{x} + \beta_n \int_{\partial K} (\mathbf{u}_h \cdot \mathbf{n}_K - \lambda_h^n)\, \mathbf{v}_h \cdot \mathbf{n}_K\, ds \\ &+ \int_K \mathbf{u}_h \cdot \nabla q_h\, d\mathbf{x} - \int_{\partial K} \lambda^n\, q_h\, ds \\ &= -\int_K f\, q_h\, d\mathbf{x}, \end{aligned} \tag{3.10}$$

for all $[\mathbf{v}_h, q_h] \in \mathcal{V}_h^k \times \mathcal{Q}_h^l$. Thus, summing the equation (3.10) on all elements K and including the global problem associated with the multiplier equation, we obtain the following mixed hybrid formulation on the partition $\mathcal{T}_h$ of the domain Ω.

Find the pair $[\mathbf{u}_h, p_h] \in \mathcal{V}_h^k \times \mathcal{Q}_h^l$ *and the Lagrange multiplier* $\lambda_h^n \in \mathcal{D}_h^k$ *such that, for all* $[\mathbf{v}_h, q_h] \in \mathcal{V}_h^k \times \mathcal{Q}_h^l$ *and* $\mu_h^n \in \mathcal{D}_h^k$

$$\sum_{K\in\mathcal{T}_h}\left[\int_K \mathbf{A}\mathbf{u}_h\cdot\mathbf{v}_h\,d\mathbf{x}+\int_K \nabla p_h\cdot\mathbf{v}_h\,d\mathbf{x}+\int_K \mathbf{u}_h\cdot\nabla q_h\,d\mathbf{x}-\int_{\partial K}\lambda_h^n\,q_h\,ds\right.$$
$$\left.+\,\beta_n\int_{\partial K}(\mathbf{u}_h\cdot\mathbf{n}_K-\lambda_h^n)\,\mathbf{v}_h\cdot\mathbf{n}_K\,ds\right] \tag{3.11}$$
$$=-\sum_{K\in\mathcal{T}_h}\int_K f\,q_h\,d\mathbf{x},$$
$$\sum_{K\in\mathcal{T}_h}\left[-\int_{\partial K}p_h\,\mu_h^n\,ds-\beta_n\int_{\partial K}(\mathbf{u}_h\cdot\mathbf{n}_K-\lambda_h^n)\,\mu_h^n\,ds\right]=0. \tag{3.12}$$

The two terms in global problem (3.12) are consistent with the pressure and flux continuities on the interface $e \in \mathcal{E}_h^0$ between two adjacent elements. The local problems (3.11) must satisfy some compatibility conditions between the velocity and pressure approximation spaces [9, 11, 12]. Therefore, based on the works of [10, 14, 19, 22, 25, 26], we add to the problem least-squares residual terms related to Darcy's law (3.1) and the mass balance (3.2) in the interior of each element K and present the stabilized primal mixed hybrid method in a compact form, as follows:

Find $\mathbf{X}_h \in \mathbf{V}_h$, *such that*

$$A_{SPHM}(\mathbf{X}_h,\mathbf{Y}_h)=F_{SPHM}(\mathbf{Y}_h),\quad \forall\ \mathbf{Y}_h\in\mathbf{V}_h \tag{3.13}$$

with $\mathbf{X}_h=[\mathbf{u}_h,p_h,\lambda_h^n]$ and $\mathbf{Y}_h=[\mathbf{v}_h,q_h,\mu_h^n]$ belonging to the product space $\mathbf{V}_h=\mathcal{V}_h^k\times\mathcal{Q}_h^l\times\mathcal{D}_h^k$ and

$$\begin{aligned}A_{SPHM}(\mathbf{X}_h,\mathbf{Y}_h)=\sum_{K\in\mathcal{T}_h}\Bigg[&\int_K\mathbf{A}\mathbf{u}_h\cdot\mathbf{v}_h\,d\mathbf{x}+\int_K\nabla p_h\cdot\mathbf{v}_h\,d\mathbf{x}+\int_K\mathbf{u}_h\cdot\nabla q_h\,d\mathbf{x}\\&+\delta_1\int_K\mathbf{K}(\mathbf{A}\mathbf{u}_h+\nabla p_h)\cdot(\mathbf{A}\mathbf{v}_h+\nabla q_h)\,d\mathbf{x}\\&+\delta_2\int_K A\,\mathrm{div}\,\mathbf{u}_h\,\mathrm{div}\,\mathbf{v}_h\,d\mathbf{x}-\int_{\partial K}\lambda_h^n\,q_h\,ds-\int_{\partial K}p_h\mu_h^n\,ds\\&+\beta_n\int_{\partial K}(\mathbf{u}_h\cdot\mathbf{n}_K-\lambda_h^n)(\mathbf{v}_h\cdot\mathbf{n}_K-\mu_h^n)\,ds\Bigg],\end{aligned} \tag{3.14}$$

$$F_{SPHM}(\mathbf{Y}_h)=\sum_{K\in\mathcal{T}_h}\left[\delta_2\int_K A\,f\ \mathrm{div}\,\mathbf{v}_h\,d\mathbf{x}-\int_K f\,q_h\,d\mathbf{x}\right], \tag{3.15}$$

where $A=\|\mathbf{A}\|_\infty$, $\|\cdot\|_\infty$ denotes the maximum norm, and the stabilization parameters δ_1 and δ_2 are related to least-squares residual forms defined in the interior of each element K. The commonly adopted values for these parameters are $\delta_1=-0.5$ and $\delta_2=0.5$, as can seen in [19, 25]. The imposition of the Neumann boundary conditions (3.3) for this formulation is made through the space (2.12) of the Lagrange multipliers on the edges/faces $e\in\mathcal{E}_h^\partial$.

3.2. Stabilized Dual Hybrid Mixed method

Here, we recall the Stabilized Dual Mixed Hybrid (SDHM) method introduced in [28]. To this, following the same steps to derive the SPHM method (3.13), but

choosing the Lagrange multiplier as the trace of the pressure field $\lambda^p = p|_e$ on each edge/face $e \in \mathcal{E}_h$ belonging to the space (2.14), we multiply the equations (3.1)-(3.2) by weighting functions, we integrate by parts the equation relative to Darcy's law, we include the least-square terms to make compatible the approximation spaces, and we introduce an edge/face stabilization parameter β_p, defined as

$$\beta_p = -\beta_n^{-1}. \tag{3.16}$$

In this context, we can present the following formulation:

Find $\mathbf{X}_h \in \mathbf{V}_h$, *such that*

$$A_{SDHM}(\mathbf{X}_h, \mathbf{Y}_h) = F_{SDHM}(\mathbf{Y}_h), \quad \forall\ \mathbf{Y}_h \in \mathbf{V}_h, \tag{3.17}$$

with $\mathbf{X}_h = [\mathbf{u}_h, p_h, \lambda_h^p]$ and $\mathbf{Y}_h = [\mathbf{v}_h, q_h, \mu_h^p]$ belonging to the product space $\mathbf{V}_h = \mathcal{V}_h^k \times \mathcal{Q}_h^l \times \mathcal{M}_h^k$ and

$$\begin{aligned} A_{SDHM}(\mathbf{X}_h, \mathbf{Y}_h) = \sum_{K\in\mathcal{T}_h} \Bigg[& \int_K \mathbf{A}\mathbf{u}_h \cdot \mathbf{v}_h \, d\mathbf{x} - \int_K p_h \operatorname{div} \mathbf{v}_h \, d\mathbf{x} - \int_K q_h \operatorname{div} \mathbf{u}_h \, d\mathbf{x} \\ & + \delta_1 \int_K \mathbf{K}(\mathbf{A}\mathbf{u}_h + \nabla p_h) \cdot (\mathbf{A}\mathbf{v}_h + \nabla q_h) \, d\mathbf{x} \\ & + \delta_2 \int_K A \operatorname{div} \mathbf{u}_h \operatorname{div} \mathbf{v}_h \, d\mathbf{x} + \int_{\partial K} \lambda_h^p \, (\mathbf{v}_h \cdot \mathbf{n}_K) \, ds \\ & + \int_{\partial K} \mu_h^p \, (\mathbf{u}_h \cdot \mathbf{n}_K) \, ds + \beta_p \int_{\partial K} (p_h - \lambda_h^p)(q_h - \mu_h^p) \, ds \Bigg], \end{aligned} \tag{3.18}$$

and $F_{SDHM}(\cdot)$ is the same of (3.15).

The terms multiplied by μ_h^p weakly impose the continuity of the normal component of the velocity field and the flux boundary condition (2.3) and enforce the continuity of the pressure field.

Remark 3.1. It's important to emphasize that the local conservation property in both methods, SPHM and SDHM, depend on the edge/face stabilization parameter. For the SDHM method, taking $\beta_p = 0$, the method becomes locally conservative [28]. On the other hand, from relation (3.16), the same behavior is observed for the SPHM method when we have $\beta_n \to \infty$. In this case, using non-conforming Raviart-Thomas spaces [6, 29] preserves the local conservation property and makes the velocity and pressure spaces compatible without incorporating least-squares residual terms.

3.3. SPHM connection with a DG method

To establish an appropriate connection between the hybrid method with an associated DG method, we rewrite the SPHM method (3.13) in terms of jumps and averages defined in (2.6)-(2.8). Thus, considering λ_h^n and μ_h^n uniquely determined on the edges/faces $e \in \mathcal{E}_h$ and the following identity

$$\begin{aligned} & \sum_{K\in\mathcal{T}_h} \int_{\partial K} (\mathbf{u}_h \cdot \mathbf{n}_K - \lambda_h^n)(\mathbf{v}_h \cdot \mathbf{n}_K - \mu_h^n) ds \\ & = \sum_{e\in\mathcal{E}_h^0} \frac{1}{2} \int_e [\![\mathbf{u}_h]\!][\![\mathbf{v}_h]\!] ds + \sum_{e\in\mathcal{E}_h^0} 2 \int_e (\{\!\{\mathbf{u}_h\}\!\} \cdot \mathbf{n}_K - \lambda_h^n) \, (\{\!\{\mathbf{v}_h\}\!\} \cdot \mathbf{n}_K - \mu_h^n) \, ds, \end{aligned} \tag{3.19}$$

we can express $A_{SPHM}(\cdot,\cdot)$ as

$$\begin{aligned} A_{SPHM}(\mathbf{X}_h,\mathbf{Y}_h) = \sum_{K\in\mathcal{T}_h}\Big[& \int_K \mathbf{A}\mathbf{u}_h\cdot\mathbf{v}_h\,d\mathbf{x} + \int_K \nabla p_h\cdot\mathbf{v}_h\,d\mathbf{x} + \int_K \mathbf{u}_h\cdot\nabla q_h\,d\mathbf{x} \\ & + \delta_1\int_K \mathbf{K}(\mathbf{A}\mathbf{u}_h+\nabla p_h)\cdot(\mathbf{A}\mathbf{v}_h+\nabla q_h)\,d\mathbf{x} \\ & + \delta_2\int_K A\,\mathrm{div}\,\mathbf{u}_h\,\mathrm{div}\,\mathbf{v}_h\,d\mathbf{x}\Big] \\ & - \sum_{e\in\mathcal{E}_h^0}\int_e \lambda_h^n\,(\llbracket q_h\rrbracket\cdot\mathbf{n}_K) + \mu_h^n\,(\llbracket p_h\rrbracket\cdot\mathbf{n}_K)\,ds \\ & + \sum_{e\in\mathcal{E}_h^0}\frac{\beta_n}{2}\int_e \llbracket\mathbf{u}_h\rrbracket\llbracket\mathbf{v}_h\rrbracket ds \\ & + \sum_{e\in\mathcal{E}_h^0} 2\beta_n\int_e (\{\!\{\mathbf{u}_h\}\!\}\cdot\mathbf{n}_K-\lambda_h^n)\,(\{\!\{\mathbf{v}_h\}\!\}\cdot\mathbf{n}_K-\mu_h^n)\,ds. \end{aligned} \tag{3.20}$$

To derive a DG method in the primal variables $\mathbf{u}_h$ and p_h related to the SPHM formulation, we can exactly solve the equation (3.12), yielding

$$\lambda_h^n = \{\!\{\mathbf{u}_h\}\!\}\cdot\mathbf{n}_K + \frac{1}{2\beta_n}\llbracket p_h\rrbracket\cdot\mathbf{n}_K \quad \text{on} \quad e\in\mathcal{E}_h^0. \tag{3.21}$$

Replacing (3.21) in (3.20) and including the linear functional $F_{SPHM}(\cdot)$ (3.15), with $\mu_h^n = 0$, we get the following discontinuous Galerkin formulation

$$\begin{aligned} & \sum_{K\in\mathcal{T}_h}\Big[\int_K \mathbf{A}\mathbf{u}_h\cdot\mathbf{v}_h\,d\mathbf{x} + \int_K \nabla p_h\cdot\mathbf{v}_h\,d\mathbf{x} + \int_K \mathbf{u}_h\cdot\nabla q_h\,d\mathbf{x} \\ & + \delta_1\int_K \mathbf{K}(\mathbf{A}\mathbf{u}_h+\nabla p_h)\cdot(\mathbf{A}\mathbf{v}_h+\nabla q_h)\,d\mathbf{x} + \delta_2\int_K A\,\mathrm{div}\,\mathbf{u}_h\,\mathrm{div}\,\mathbf{v}_h\,d\mathbf{x}\Big] \\ & + \sum_{e\in\mathcal{E}_h^0}\int_e (\llbracket p_h\rrbracket\cdot\{\!\{\mathbf{v}_h\}\!\} + \{\!\{\mathbf{u}_h\}\!\}\cdot\llbracket q_h\rrbracket)\,ds + \tau_p\sum_{e\in\mathcal{E}_h^0}\int_e \llbracket p_h\rrbracket\cdot\llbracket q_h\rrbracket ds \\ & + \tau_u\sum_{e\in\mathcal{E}_h^0}\int_e \llbracket\mathbf{u}_h\rrbracket\llbracket\mathbf{v}_h\rrbracket\,ds \\ = & \sum_{K\in\mathcal{T}_h}\Big[\delta_2\int_K A\,f\ \mathrm{div}\,\mathbf{v}_h\,d\mathbf{x} - \int_K f\,q_h\,d\mathbf{x}\Big]. \end{aligned} \tag{3.22}$$

In this case, $\tau_p = -1/(2\beta_n)$ and $\tau_u = 2\beta_n$. The DG method derived is consistent due to transmission conditions $\llbracket\mathbf{u}\rrbracket = 0$ and $\llbracket p\rrbracket = \mathbf{0}$. Moreover, setting $\delta_2 = \tau_u = 0$ and $\delta_1 = -1/2$, we recover a stabilized mixed DG method proposed and analyzed in [22].

Remark 3.2. Similarly, from the SDHM method (3.17), adopting discontinuous interpolations for the Lagrange multiplier ($\lambda_h^p \in \mathcal{D}_h^k$), we can derive the following relation for the Lagrange multiplier

$$\lambda_h^p = \{\!\{p_h\}\!\} - \frac{1}{2\beta_p}\llbracket\mathbf{u}_h\rrbracket \quad \text{on} \quad e\in\mathcal{E}_h^0, \tag{3.23}$$

where integrating by parts the terms $(p_h, \operatorname{div} \mathbf{v}_h)$ and $(q_h, \operatorname{div} \mathbf{u}_h)$ and using the definition (3.16), we recover the same DG method associated with the SPHM method (3.22), setting $\tau_p = 2\beta_p$ and $\tau_u = -\dfrac{1}{2\beta_p}$.

4. Numerical analysis

The numerical analysis of hybrid methods typically relies on arguments similar to those employed in the analysis of discontinuous Galerkin methods. These arguments involve employing norms defined at the element level, incorporating jumps and averages of variables along edges/faces, and utilizing specific inequalities such as trace and generalized Poincaré inequalities [8,25]. Therefore, the numerical analysis of the SPHM formulation presented in (3.13) is performed using the bilinear form $A_{SPHM}(\cdot,\cdot)$, which is reformulated in terms of jumps and averages as shown in (3.20). In this context, first, we demonstrate the consistency of the proposed hybrid method.

4.1. Consistency

Lemma 4.1. *The stabilized primal mixed hybrid formulation* (3.13) *is consistent, that is, the exact solution* $\mathbf{X} = [\mathbf{u}, p, \lambda^n]$ *satisfies*

$$A_{SPHM}(\mathbf{X}, \mathbf{Y}_h) = F_{SPHM}(\mathbf{Y}_h), \quad \forall\ \mathbf{Y}_h \in \mathbf{V}_h. \tag{4.1}$$

Proof. *From the SPHM method, with* $A_{SPHM}(\cdot,\cdot)$ *in the form presented in* (3.20), *let the triple* $[\mathbf{u}, p, \lambda^n]$, *with* $\mathbf{u}$ *and* p *solution of the model problem* (2.1)-(2.2) *and* $\lambda^n = \mathbf{u}\cdot\mathbf{n}_K|_e$ *on each edge/face* $e \in \mathcal{E}_h$, *such that satisfies*

$$\begin{aligned}
&\sum_{K\in\mathcal{T}_h}\Big[\int_K \mathbf{A}\mathbf{u}\cdot\mathbf{v}_h\,d\mathbf{x} + \int_K \nabla p\cdot\mathbf{v}_h\,d\mathbf{x} + \int_K \mathbf{u}\cdot\nabla q_h\,d\mathbf{x}\\
&+\delta_1\int_K \mathbf{K}(\mathbf{A}\mathbf{u}_h+\nabla p_h)\cdot(\mathbf{A}\mathbf{v}_h+\nabla q_h)\,d\mathbf{x} + \delta_2\int_K A\operatorname{div}\mathbf{u}\operatorname{div}\mathbf{v}_h\,d\mathbf{x}\Big]\\
&-\sum_{e\in\mathcal{E}_h^0}\int_e \lambda^n\,([\![q_h]\!]\cdot\mathbf{n}_K) + \mu_h^n\,([\![p]\!]\cdot\mathbf{n}_K)\,ds + \sum_{e\in\mathcal{E}_h^0}\frac{\beta_n}{2}\int_e [\![\mathbf{u}]\!][\![\mathbf{v}_h]\!]ds\\
&+\sum_{e\in\mathcal{E}_h^0} 2\beta_n\int_e (\{\!\{\mathbf{u}\}\!\}\cdot\mathbf{n}_K - \lambda^n)\,(\{\!\{\mathbf{v}_h\}\!\}\cdot\mathbf{n}_K - \mu_h^n)\,ds,
\end{aligned} \tag{4.2}$$

for all $[\mathbf{v}_h, q_h, \mu_h^n] \in \mathcal{V}_h^k \times \mathcal{Q}_h^l \times \mathcal{D}_h^k$. *From the exact solution* $\mathbf{X} = [\mathbf{u}, p, \lambda^n]$ *and considering the transmission conditions* (3.4), *the system* (4.2) *reduces to*

$$\begin{aligned}
&\sum_{K\in\mathcal{T}_h}\int_K \mathbf{A}\mathbf{u}\cdot\mathbf{v}_h\,d\mathbf{x} + \int_K \nabla p\cdot\mathbf{v}_h\,d\mathbf{x} + \int_K \mathbf{u}\cdot\nabla q_h\,d\mathbf{x} - \sum_{K\in\mathcal{T}_h}\int_{\partial K}(\mathbf{u}\cdot\mathbf{n}_K)\,q_h\,ds\\
&= -\sum_{K\in\mathcal{T}_h}\int_K f\,q_h\,d\mathbf{x}
\end{aligned}$$

which integrated by parts leads to

$$\sum_{K\in\mathcal{T}_h}\int_K [\mathbf{A}\mathbf{u} + \nabla p]\cdot\mathbf{v}_h\,d\mathbf{x} = 0, \quad \forall \mathbf{v}_h \in \mathcal{V}_h^k, \tag{4.3}$$

$$\sum_{K\in\mathcal{T}_h}\int_K [\operatorname{div}\mathbf{u}-f]\; q_h\, d\mathbf{x}=0,\quad \forall q_h\in\mathcal{Q}_h^l, \tag{4.4}$$

and the proof is complete. □

4.2. Existence and uniqueness

To prove the existence and uniqueness of the SPHM formulation (3.13), we define the mesh dependent norm $\|\cdot\|_{SH}$, to prove stability of the bilinear form $A_{SPHM}(\cdot,\cdot)$ presented in (3.20), as follows

$$\|\mathbf{X}_h\|_{SH}^2=|[\mathbf{u}_h,p_h]|_{\mathcal{T}_h}^2+|[\mathbf{u}_h,p_h,\lambda_h^n]|_{\partial\mathcal{T}_h}^2 \tag{4.5}$$

where

$$\begin{aligned}|[\mathbf{u}_h,p_h]|_{\mathcal{T}_h}^2=\sum_{K\in\mathcal{T}_h}\Big[&\int_K \mathbf{A}\mathbf{u}_h\cdot\mathbf{u}_h\,d\mathbf{x}+\int_K \mathbf{K}\nabla p_h\cdot\nabla p_h\,d\mathbf{x}\\&+\int_K A|\operatorname{div}\mathbf{u}_h|^2\,d\mathbf{x}\Big],\end{aligned} \tag{4.6}$$

$$\begin{aligned}|[\mathbf{u}_h,p_h,\lambda_h^n]|_{\partial\mathcal{T}_h}^2=\sum_{e\in\mathcal{E}_h^0}\Big[&\frac{\beta_n}{2}\int_e|[\![\mathbf{u}_h]\!]|^2ds+2\beta_n\int_e|\{\!\{\mathbf{u}_h\}\!\}\cdot\mathbf{n}_K-\lambda_h^n|^2ds\\&+\frac{1}{2\beta_n}\int_e|[\![p_h]\!]|^2ds\Big].\end{aligned} \tag{4.7}$$

4.2.1. Global stability

Using the norm (4.5), the next Lemma establishes the stability of the form (3.20) in the sense of Babuška [9].

Lemma 4.2 (SPHM global inf-sup stability)**.** *There exists a positive constant* $\gamma>0$*, independent of the mesh size, such that*

$$\sup_{\mathbf{Y}_h\in\mathbf{V}_h}\frac{A_{SPHM}(\mathbf{X}_h,\mathbf{Y}_h)}{\|\mathbf{Y}_h\|_{SH}}\geq\gamma\|\mathbf{X}_h\|_{SH},\quad\forall\ \mathbf{X}_h\in\mathbf{V}_h. \tag{4.8}$$

Proof. *Setting* $\delta_1=-1/2$*,* $\delta_2=1/2$*, and choosing* $\bar{\mathbf{Y}}_h=[\bar{\mathbf{v}}_h,\bar{q}_h,\bar{\mu}_h^n]$ *with*

$$\bar{\mathbf{v}}_h=\mathbf{u}_h,\quad \bar{q}_h=-p_h,\quad \bar{\mu}_h^n=\lambda_h^n-\frac{1}{2\beta_n}[\![p_h]\!]\cdot\mathbf{n}_K \tag{4.9}$$

such that

$$\|\bar{\mathbf{Y}}_h\|_{SH}\leq 2\|\mathbf{X}_h\|_{SH}, \tag{4.10}$$

for any $\mathbf{X}_h\in\mathbf{V}_h$*, we have*

$$\begin{aligned}&A_{SPHM}(\mathbf{X}_h,\bar{\mathbf{Y}}_h)\\&\geq\frac{1}{2}|[\mathbf{u}_h,p_h]|_{\mathcal{T}_h}^2+\sum_{e\in\mathcal{E}_h}\Big[\frac{\beta_n}{2}\int_e|[\![\mathbf{u}_h]\!]|^2ds+2\beta_n\int_e|\{\!\{\mathbf{u}_h\}\!\}\cdot\mathbf{n}_K-\lambda_h^n|^2ds\\&\quad+\frac{1}{2\beta_n}\int_e|[\![p_h]\!]|^2ds+\int_e|[\![p_h]\!]\cdot\mathbf{n}_K(\{\!\{\mathbf{u}_h\}\!\}\cdot\mathbf{n}_K-\lambda_h^n)|\,ds\Big].\end{aligned} \tag{4.11}$$

Considering that

$$|[\![p_h]\!]\cdot\mathbf{n}_K(\{\!\{\mathbf{u}_h\}\!\}\cdot\mathbf{n}_K-\lambda_h^n)|\geq-\frac{1}{2}\left(\frac{1}{2\beta_n}|[\![p_h]\!]|^2+2\beta_n|(\{\!\{\mathbf{u}_h\}\!\}\cdot\mathbf{n}_K-\lambda_h^n)|^2\right) \tag{4.12}$$

we get

$$A_{SPHM}(\mathbf{X}_h,\bar{\mathbf{Y}}_h)\geq\frac{1}{2}\left(|[\mathbf{u}_h,p_h]|^2_{\mathcal{T}_h}+|[\mathbf{u}_h,p_h,\lambda_h^n]|^2_{\partial\mathcal{T}_h}\right)=\frac{1}{2}\|\mathbf{X}_h\|^2_{SH}. \tag{4.13}$$

Thus,

$$\sup_{\mathbf{Y}_h\in\mathbf{V}_h}\frac{A_{SPHM}(\mathbf{X}_h,\mathbf{Y}_h)}{\|\mathbf{Y}_h\|_{SH}}\geq\frac{A_{SPHM}(\mathbf{X}_h,\bar{\mathbf{Y}}_h)}{\|\bar{\mathbf{Y}}_h\|_{SH}}\geq\frac{1}{4}\|\mathbf{X}_h\|_{SH}$$

which proves the lemma, with $\gamma=1/4$, and the stability of the proposed SPHM formulation. □

4.2.2. Continuity

Continuity or boundedness of $A_{SPHM}(\cdot,\cdot)$ is proved in the same norm of the stability (4.5), but in the infinite dimension space $\mathbf{V}(\mathcal{T}_h)=\mathcal{V}(\mathcal{T}_h)\times\mathcal{Q}(\mathcal{T}_h)\times\mathcal{D}(\mathcal{E}_h)$ with

$$\begin{aligned}
\mathcal{V}(\mathcal{T}_h)&=\{\mathbf{v}\in[L^2(\Omega)]^d;\mathbf{v}|_K\in[H^1(K)]^d,\ \forall K\in\mathcal{T}_h\},\\
\mathcal{Q}(\mathcal{T}_h)&=\{q\in L^2(\Omega);q|_K\in H^1(K),\ \forall K\in\mathcal{T}_h\},\\
\mathcal{D}(\mathcal{E}_h)&=\{\mu|_e\in L^2(e),\ \forall e\in\mathcal{E}_h^0,\ \mu|_e=0,\ \forall e\in\mathcal{E}_h^\partial\}.
\end{aligned}$$

Lemma 4.3 (Continuity of $A_{SPHM}(\cdot,\cdot)$ and $F_{SPHM}(\cdot)$)**.** *There exist constants $M_C<\infty$ and $M_F<\infty$, independent of the mesh size, such that*

$$|A_{SPHM}(\mathbf{X},\mathbf{Y})|\leq M_C\|\mathbf{X}\|_{SH}\|\mathbf{Y}\|_{SH},\quad\forall\ \mathbf{X},\mathbf{Y}\in\mathbf{V}(\mathcal{T}_h), \tag{4.14}$$

$$|F_{SPHM}(\mathbf{Y})|\leq M_F\|\mathbf{Y}\|_{SH},\qquad\forall\ \mathbf{Y}\in\mathbf{V}(\mathcal{T}_h). \tag{4.15}$$

Proof. *To prove the continuity of $A_{SPHM}(\cdot,\cdot)$ defined in* (3.20)*, we apply the triangle inequality to obtain*

$$\begin{aligned}
|A_{SPHM}(\mathbf{X},\mathbf{Y})|\leq&C|[\mathbf{u},p]|_{\mathcal{T}_h}|[\mathbf{v},q]|_{\mathcal{T}_h}+\left|\sum_{e\in\mathcal{E}_h^0}\frac{\beta_n}{2}\int_e[\![\mathbf{u}]\!][\![\mathbf{v}]\!]ds\right|\\
&+\left|\sum_{e\in\mathcal{E}_h^0}2\beta_n\int_e\left(\{\!\{\mathbf{u}\}\!\}\cdot\mathbf{n}_K-\lambda^n\right)\left(\{\!\{\mathbf{v}\}\!\}\cdot\mathbf{n}_K-\mu^n\right)ds\right|\\
&+\left|\sum_{e\in\mathcal{E}_h^0}\int_e\lambda^n\left([\![q]\!]\cdot\mathbf{n}_K\right)ds\right|+\left|\sum_{e\in\mathcal{E}_h^0}\int_e\mu^n\left([\![p]\!]\cdot\mathbf{n}_K\right)ds\right|.
\end{aligned} \tag{4.16}$$

If we set $\delta_2=-\delta_1=1/2$, the constant C is $1/2$. The all terms in (4.16)*, except the two last terms, are bounded by $|[\mathbf{u},p,\lambda^n]|_{\partial\mathcal{T}_h}|[\mathbf{v},q,\mu^n]|_{\partial\mathcal{T}_h}$. Thus, we rewrite these terms as*

$$\left|\sum_{e\in\mathcal{E}_h^0}\int_e\lambda^n\left([\![q]\!]\cdot\mathbf{n}_K\right)ds\right|=\left|\sum_{e\in\mathcal{E}_h^0}\int_e(\lambda^n-\{\!\{\mathbf{u}\}\!\}\cdot\mathbf{n}_K+\{\!\{\mathbf{u}\}\!\}\cdot\mathbf{n}_K)\left([\![q]\!]\cdot\mathbf{n}_K\right)ds\right|$$

$$\leq \left| \sum_{e\in\mathcal{E}_h^0} \int_e (\lambda^n - \{\!\{\mathbf{u}\}\!\}\cdot\mathbf{n}_K)\,([\![q]\!]\cdot\mathbf{n}_K)\,ds \right| + \left| \sum_{e\in\mathcal{E}_h^0} \int_e \{\!\{\mathbf{u}\}\!\}\cdot[\![q]\!]\,ds \right|. \tag{4.17}$$

To estimate the last term in (4.17)*, we employ the inequality* (2.9)*, integration by parts and the generalized Poincaré inequality (see [4])*

$$\sum_{K\in\mathcal{T}_h}\int_K |q|^2\,d\mathbf{x} \leq C_K\left(\sum_{K\in\mathcal{T}_h}\int_K |\nabla q|^2\,d\mathbf{x} + h^{-1}\sum_{e\in\mathcal{E}_h^0}\int_e |[\![q]\!]|^2 ds\right) \tag{4.18}$$

to get

$$\begin{aligned}
&\left| \sum_{e\in\mathcal{E}_h^0} \int_e \{\!\{\mathbf{u}\}\!\}\cdot[\![q]\!]\,ds \right| \\
&\leq \left| \sum_{K\in\mathcal{T}_h} \int_{\partial K} q(\mathbf{u}\cdot\mathbf{n}_K) ds \right| \\
&= \left| \sum_{K\in\mathcal{T}_h} \int_K (\mathbf{u}\cdot\nabla q + q\,\mathrm{div}\,\mathbf{u})\,d\mathbf{x} \right| \\
&\leq |\mathbf{u}|_{0,h}|q|_{1,h} + C_K\left(|q|_{1,h}^2 + 2A\beta_0\sum_{e\in\mathcal{E}_h^0}\frac{1}{2\beta_n}\int_e |[\![q]\!]|^2 ds\right)^{1/2} |\,\mathrm{div}\,\mathbf{u}|_{0,h}.
\end{aligned} \tag{4.19}$$

Thus, the estimative (4.14) *is proved combining* (4.17) *and* (4.19) *with* (4.16)*, with* M_C *depending on stabilization parameters* δ*'s and* β_0 *and the constant* C_K *of the generalized Poincaré inequality* (4.18)*.*

In the same way, using the generalized Poincaré inequality (4.18)*, we can prove the continuity of* $F_{SPHM}(\cdot)$

$$|F_{SPHM}(\mathbf{Y})| \leq \left| \sum_{K\in\mathcal{T}_h} \delta_2 \int_K A\,f\ \mathrm{div}\,\mathbf{v}\,d\mathbf{x} \right| + \left| \sum_{K\in\mathcal{T}_h}\int_K f\,q\,d\mathbf{x} \right| \leq M_F\|\mathbf{Y}\|_{SH}. \tag{4.20}$$

The proof is complete with M_F *depending on* δ_2*,* β_0*,* $\|f\|_{0,h}$ *and the constant of the generalized Poincaré inequality* (4.18)*.* □

4.3. Energy norm error estimates

The exact solution $\mathbf{X} = [\mathbf{u}, p, \lambda^n]$ of the Darcy problem and the SPHM consistency (Lemma 4.1) leads to the orthogonality property

$$A_{SPHM}(\mathbf{X} - \mathbf{X}_h, \mathbf{Y}_h) = 0, \quad \forall\ \mathbf{Y}_h \in \mathbf{V}_h. \tag{4.21}$$

Let $\tilde{\mathbf{X}} \in \mathbf{V}_h$ be appropriate projections of $\mathbf{u}$, p and λ^n on $\mathcal{V}_h^k$, $\mathcal{Q}_h^l$ and $\mathcal{D}_h^k$, respectively. Thus, from Lemma 4.2, it follows that

$$\gamma\|\tilde{\mathbf{X}} - \mathbf{X}_h\|_{SH} \leq \frac{A_{SPHM}(\tilde{\mathbf{X}} - \mathbf{X}_h, \tilde{\mathbf{Y}} - \overline{\mathbf{Y}}_h)}{\|\tilde{\mathbf{Y}} - \overline{\mathbf{Y}}_h\|_{SH}},$$

choosing $\overline{\mathbf{Y}}_h = [\mathbf{u}_h, -p_h, \lambda_h^n - \frac{1}{2\beta_n}[\![p_h]\!]\cdot\mathbf{n}_K]$ and $\tilde{\mathbf{Y}} = [\tilde{\mathbf{u}}, -\tilde{p}, \tilde{\lambda}^n - \frac{1}{2\beta_n}[\![\tilde{p}]\!]\cdot\mathbf{n}_K]$ and considering (4.10) we have

$$\begin{aligned}\frac{1}{2}\|\tilde{\mathbf{X}} - \mathbf{X}_h\|_{SH}^2 \leq & A_{SPHM}(\tilde{\mathbf{X}} - \mathbf{X}_h, \tilde{\mathbf{X}} - \mathbf{X}_h)\\ \leq & A_{SPHM}(\tilde{\mathbf{X}} - \mathbf{X}, \tilde{\mathbf{X}} - \mathbf{X}_h) + A_{SPHM}(\mathbf{X} - \mathbf{X}_h, \tilde{\mathbf{X}} - \mathbf{X}_h).\end{aligned}$$

Considering orthogonality (4.21) and continuity of $A_{SPHM}(\cdot,\cdot)$ (Lemma 4.3), we get

$$\|\tilde{\mathbf{X}} - \mathbf{X}_h\|_{SH} \leq 2M_C\|\tilde{\mathbf{X}} - \mathbf{X}\|_{SH}. \tag{4.22}$$

Using the triangle inequality and the result (4.22), we obtain

$$\begin{aligned}\|\mathbf{X} - \mathbf{X}_h\|_{SH} \leq & \|\mathbf{X} - \tilde{\mathbf{X}}\|_{SH} + \|\tilde{\mathbf{X}} - \mathbf{X}_h\|_{SH}\\ \leq & (1 + 2M_C)\|\mathbf{X} - \tilde{\mathbf{X}}\|_{SH}.\end{aligned} \tag{4.23}$$

Considering $\tilde{\mathbf{u}} = \mathbf{u}_I$, $\tilde{p} = p_I$ and $\tilde{\lambda}^n = \lambda_I^n$ the continuous interpolants of $\mathbf{u}$, p and λ^n, respectively, the definition of the Lagrange multiplier $\lambda^n = \mathbf{u}\cdot\mathbf{n}_K|_e$ on each edge/face $e \in \mathcal{E}_h^0$, and the norm (4.5), the estimate (4.23) reduces to

$$\|\mathbf{X} - \mathbf{X}_h\|_{SH} \leq (1 + 2M_C)|[\mathbf{u} - \mathbf{u}_I, p - p_I]|_{\mathcal{T}_h} \tag{4.24}$$

since, in this case, $\lambda_I^n = \mathbf{u}_I\cdot\mathbf{n}_K|_e$ on each edge/face $e \in \mathcal{E}_h^0$ and the jumps of $p - p_I$ and $\mathbf{u} - \mathbf{u}_I$ are zero at the interelement boundaries. Therefore, assuming $\|\operatorname{div}\mathbf{u}\|_{0,K} \leq C\|\nabla\mathbf{u}\|_{0,K}$, using the approximation properties of the interpolant, adopting equal order approximations for velocity, pressure, and the multiplier ($k = l$), and supposing sufficiently regular solutions ($\mathbf{u} \in [H^{k+1}]^d$, $p \in H^{k+1}$) we derive the following rate of convergence in the energy norm

$$\|\mathbf{X} - \mathbf{X}_h\|_{SH} \leq Ch^k\left(|\mathbf{u}|_{k+1} + |p|_{k+1}\right). \tag{4.25}$$

The coefficients of stability, continuity, and interpolant are encapsulated in the constant C.

A discussion of convergence rates in L^2-norm, for different choices of the stabilization parameters δ's and β, can be seen in [25].

Remark 4.1. Using the same arguments employed for the SPHM method, the consistency, existence, uniqueness, and error estimates of the SDHM method (3.17) can be proved in a similar norm adopted in (4.5), with $|[\mathbf{u}_h, p_h, \lambda_h^p]|_{\partial\mathcal{T}_h}$ in the place of (4.7) defined as

$$\begin{aligned}&|[\mathbf{u}_h, p_h, \lambda_h^p]|_{\partial\mathcal{T}_h}^2\\ &= \sum_{e\in\mathcal{E}_h^0}\left[\frac{1}{2\beta_p}\int_e |[\![\mathbf{u}_h]\!]|^2 ds + 2\beta_p\int_e |\,\{\!\{p_h\}\!\} - \lambda_h^p|^2 ds + \frac{\beta_p}{2}\int_e |[\![p_h]\!]|^2 ds\right]\end{aligned}$$

and replacing $\bar{\mu}_h^n$ by $\bar{\mu}_h^p = -\lambda_h^p + \frac{1}{2\beta_p}[\![\mathbf{u}_h]\!]$ in (4.9) to demonstrate the global inf-sup stability. Moreover, this analysis is also valid for the continuous interpolations for the Lagrange multiplier.

5. Computational implementation

To solve the SPHM and SDHM formulations, we apply the static condensation strategy to eliminate the velocity and pressure degrees-of-freedom at the element level in favor of the Lagrange multiplier, generating a global system involving only degrees of freedom of the multiplier. However, to employ this strategy, the local problems must have a unique solution. In particular, the SPHM method does not satisfy this requirement because the pressure field is only determined up to an arbitrary additive constant. Therefore, to overcome this, we add a global unknown, a constant-pressure mode associated with a null mean value of the pressure field over each element K, to make the local problems solvable. To this, we introduce in the SPHM system a new global variable $\bar{p}_h \in P_h^0 = \{\bar{p} \in L^2(\Omega); \bar{p}|_K \in \mathbb{Q}_0(K),\ \forall K \in \mathcal{T}_h\}$, associated to constant-pressure mode, through the following consistent and symmetric term

$$\left(\bar{p}_h - \int_K p_h \, d\mathbf{x}\right)\left(\bar{q}_h - \int_K q_h \, d\mathbf{x}\right) = 0, \quad \forall [\bar{q}_h, q_h] \in P_h^0 \times \mathcal{Q}_h^l. \tag{5.1}$$

5.1. The local problems

The local problem associated with the SPHM method (3.13), adding the term (5.1) to ensure the solvability of the local problems, can be written in the following bilinear forms

$$\begin{aligned} a_K([\mathbf{u}_h, p_h], [\mathbf{v}_h, q_h]) = &\int_K \mathbf{A}\mathbf{u}_h \cdot \mathbf{v}_h \, d\mathbf{x} + \int_K \nabla p_h \cdot \mathbf{v}_h \, d\mathbf{x} + \int_K \mathbf{u}_h \cdot \nabla q_h \, d\mathbf{x} \\ &+ \delta_1 \int_K \mathbf{K}(\mathbf{A}\mathbf{u}_h + \nabla p_h) \cdot (\mathbf{A}\mathbf{v}_h + \nabla q_h) \, d\mathbf{x} \\ &+ \delta_2 \int_K A \operatorname{div} \mathbf{u}_h \operatorname{div} \mathbf{v}_h \, d\mathbf{x} + \int_K p_h \, d\mathbf{x} \int_K q_h \, d\mathbf{x} \\ &+ \beta_n \int_{\partial K} (\mathbf{u}_h \cdot \mathbf{n}_K)(\mathbf{v}_h \cdot \mathbf{n}_K) \, ds, \end{aligned} \tag{5.2}$$

$$\begin{aligned} b_K([\lambda_h^n, \bar{p}_h], [\mathbf{v}_h, q_h]) = &- \int_{\partial K} \lambda_h^n \, q_h \, ds - \beta_n \int_{\partial K} \lambda_h^n (\mathbf{v}_h \cdot \mathbf{n}_K) \, ds \\ &- \bar{p}_h \int_K q_h \, d\mathbf{x}, \end{aligned} \tag{5.3}$$

and the linear functional

$$f_K([\mathbf{v}_h, q_h]) = \delta_2 \int_K A f \operatorname{div} \mathbf{v}_h \, d\mathbf{x} - \int_K f \, q_h \, d\mathbf{x}. \tag{5.4}$$

Then, the local problem can be presented as

$$a_K([\mathbf{u}_h, p_h], [\mathbf{v}_h, q_h]) + b_K([\lambda_h^n, \bar{p}_h], [\mathbf{v}_h, q_h]) = f_K([\mathbf{v}_h, q_h]). \tag{5.5}$$

Considering $\mathbf{A}_K$ and $\mathbf{B}_K$ the matrices generated by the local bilinear operators $a_K(\cdot,\cdot)$ and $b_K(\cdot,\cdot)$, respectively, and $\mathbf{F}_K$ the vector originating from $f_K(\cdot)$, we can rewrite the local problem (5.5) in a matrix form

$$\mathbf{A}_K \mathbf{U} + \mathbf{B}_K \mathbf{\Lambda} = \mathbf{F}_K, \quad \forall K \in \mathcal{T}_h. \tag{5.6}$$

Given that $\mathbf{A}_K$ is invertible, we solve the system (5.6) to obtain

$$\mathbf{U} = \mathbf{A}_K^{-1}(\mathbf{F}_K - \mathbf{B}_K \mathbf{\Lambda}), \quad \forall K \in \mathcal{T}_h. \tag{5.7}$$

5.2. The global problem

From the system (3.13), we define the bilinear form

$$c_K([\lambda_h^n, \bar{p}_h], [\mu_h^n, \bar{q}_h]) = \beta \int_{\partial K} \lambda_h \, \mu_h \, ds + \bar{p}_h \, \bar{q}_h.$$

Considering $\mathbf{B}_K^T$ and $\mathbf{C}_K$ the matrices given by the bilinear forms $b_K([\mu_h^n, \bar{q}_h], [\mathbf{u}_h, p_h])$ and $c_K([\lambda_h^n, \bar{p}_h], [\mu_h^n, \bar{q}_h]$, respectively, we can write the global problem in a matrix form as follows

$$\sum_{K \in \mathcal{T}_h} \mathbf{B}_K^T \mathbf{U} + \sum_{K \in \mathcal{T}_h} \mathbf{C}_K \mathbf{\Lambda} = \mathbf{0}. \tag{5.8}$$

Replacing (5.7) in (5.8) we obtain the global system in the multiplier only as

$$\sum_{K \in \mathcal{T}_h} (\mathbf{C}_K - \mathbf{B}_K^T \mathbf{A}_K^{-1} \mathbf{B}_K) \mathbf{\Lambda} = - \sum_{K \in \mathcal{T}_h} \mathbf{B}_K^T \mathbf{A}_K^{-1} \mathbf{F}_K. \tag{5.9}$$

After solving the global system (5.9), the vector $\mathbf{U}$ is obtained by post-processing $\mathbf{\Lambda}$, given by (5.9), in (5.7).

We follow the same steps above to apply the static condensation for the SDHM method (3.17), but, in this case, it is not necessary to include the term (5.1). It is important to emphasize that adding the term (5.1) to the SPHM method increases the dimension of the global problem by one degree of freedom per element compared with the SDHM method.

6. Numerical results

In this section are presented several numerical studies in two and three dimensions, considering homogeneous and heterogeneous porous media, comparing the proposed SPHM method with the SDHM method adopting three approaches:

- SPHM method using standard polynomial basis, as Lagrange or Legendre, for the primal variables and discontinuous interpolations for the Lagrange multipliers, named SPHM-D;
- SPHM method employing Raviart-Thomas spaces for the velocity field, the standard polynomial basis for the pressure, and discontinuous interpolations for the Lagrange multipliers, called SPHM-RT;
- SDHM method applying standard polynomial basis for the velocity and pressure fields and continuous interpolations for the Lagrange multipliers, called SDHM-C;

As shown, employing specific choices for the stabilization parameters, SPHM and SDHM methods generate the same DG method (see Remark 3.2). Therefore, in these numerical studies, the SDHM method with discontinuous multipliers is not considered because the results are the same as those obtained by the SPHM method. Moreover, a study about local conservation of the proposed hybrid methods is presented and compared with the results of classical Raviart-Thomas conservative spaces. Finally, we assess the computational cost associated with solving these formulations and present the performance of two preconditioners: Jacobi and SSOR.

The numerical results presented in this section have been carried out with a code written in C++ with the support of the `deal.II` library [3]. All the tests were run on a MacBook Pro with a 2.8 GHz Intel Core i7 Quad-Core and 16 GB of RAM. To solve the linear system, we employ the Conjugate Gradient (CG) method combined with SSOR preconditioner adopting a 10^{-9} tolerance, and the local problems are solved by applying the Gauss-Jordan method to invert the matrix $\mathbf{A}_K$. Convergence studies adopt square or cubic domains composed of quadrilateral or hexahedral grids with 2^n elements in each direction, where $n = 2, 3, 4, 5, 6$, with polynomial orders $k = l = 1, 2, 3$. The least-squares stabilization parameters considered are $\delta_1 = -0.5$ and $\delta_2 = 0.5$, and the interface stabilization parameter is $\beta_0 = 1.0$ for SPHM-D and SDHM-C methods. On the other hand, the SPHM-RT method is fixed $\delta_1 = \delta_2 = 0$ and $\beta_0 = 1.0/h^3$. To generate fairer comparisons between methods that use continuous or discontinuous multipliers, the convergence results are presented in terms of the global degrees of freedom associated with the Lagrange multipliers ($\#dof$), which are divided by the dimension d to obtain the correct slope of the convergence rate. Moreover, the boundary conditions are imposed using the analytical solutions of the numerical examples studied.

6.1. Homogeneous medium

In this section, the hybrid methods SPHM-D, SPHM-RT, and SDHM-C are tested in two and three dimensions, adopting uniform meshes of quadrilateral or hexahedral elements in homogeneous porous media.

6.1.1. Numerical test Case 1

The first numerical study is performed in a two-dimensional square domain $\Omega = [-1, 1]^2$ with $\mathbf{K} = \mathbf{I}$ adopting the analytical solution

$$p = 2\sin(\pi x)\sin(\pi y). \tag{6.1}$$

Figure 1 presents a h-convergence study of velocity, divergence, and pressure. The results demonstrate convergence rates of $O(h^{k+1})$ for all velocity, divergence, and pressure approximations, except for the velocity field approximated with the SDHM-C method using $k = l = 2$ (see Fig. 1(b)). The approximate velocity field by the SDHM-C method proved more accurate than the other hybrid approaches for $k = l = 1$ (see Fig. 1(a)). For biquadratic and bicubic elements, SPHM-RT was the most accurate. The SDHM-C method is more accurate for divergence and pressure fields than the SPHM-D and SPHM-RT methods.

6.1.2. Numerical test Case 2

The next convergence test is developed in a three-dimensional domain $\Omega = [-1, 1]^3$ considering isotropic hydraulic conductivity $\mathbf{K} = \mathbf{I}$ and the following analytical solution for the pressure field

$$p = 2\sin(\pi x)\sin(\pi y)\sin(\pi z). \tag{6.2}$$

The results of this convergence study can be seen in Figure 2. In this three-dimensional example, it is possible to verify optimal convergence rates for divergence and pressure fields in all simulations performed. Again, the SDHM-C method is the

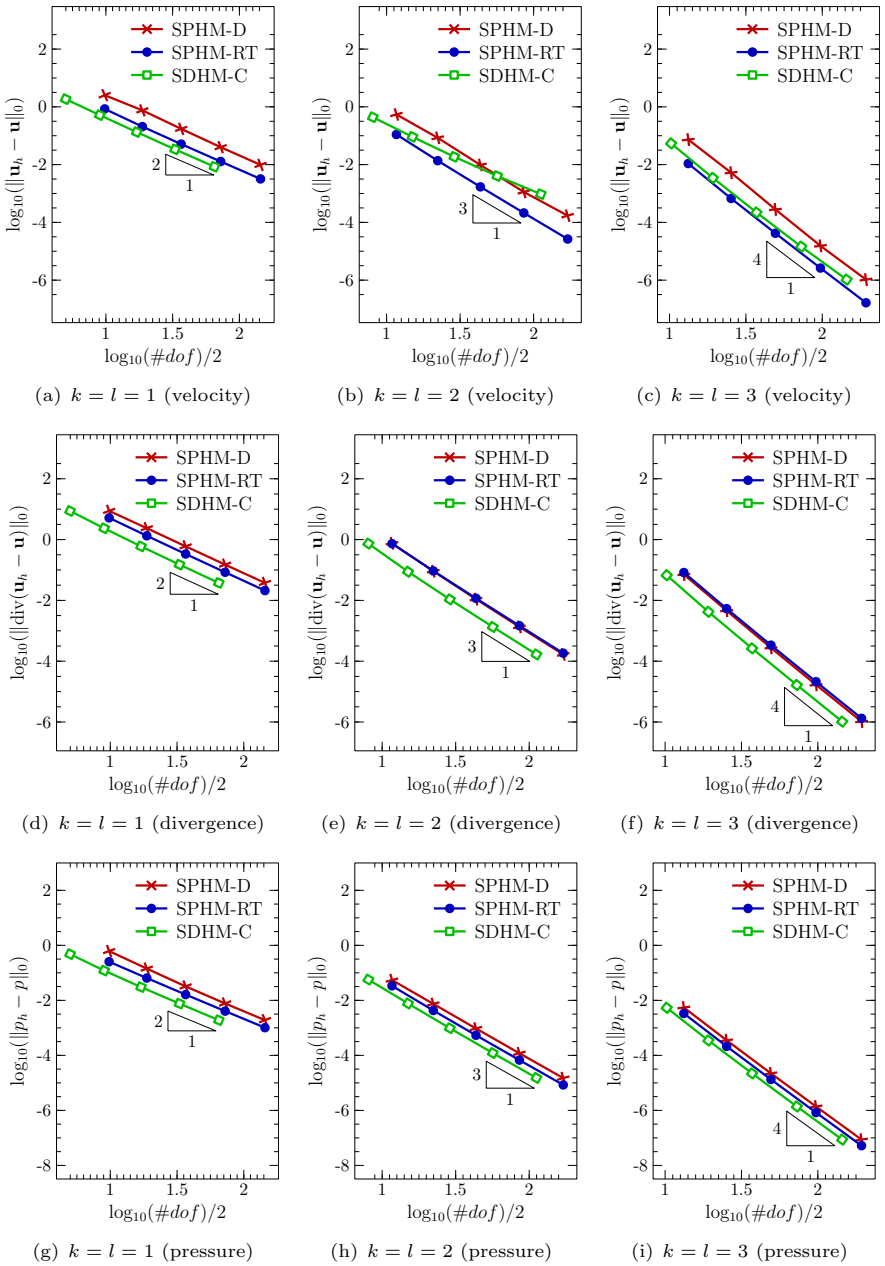

(a) $k = l = 1$ (velocity) (b) $k = l = 2$ (velocity) (c) $k = l = 3$ (velocity)

(d) $k = l = 1$ (divergence) (e) $k = l = 2$ (divergence) (f) $k = l = 3$ (divergence)

(g) $k = l = 1$ (pressure) (h) $k = l = 2$ (pressure) (i) $k = l = 3$ (pressure)

Figure 1. Numerical test case 1: h-convergence studies of the velocity (top), divergence (middle), and pressure (bottom) comparing SPHM-D, SPHM-RT, and SDHM-C in L^2-norm in terms of degrees of freedom.

most accurate regarding the degrees of freedom for the divergence and pressure approximations and bilinear elements for the velocity field. Moreover, For the velocity field, the convergence rates obtained by the SPHM-D and SPHM-RT methods tend to the optimal rate $O(h^{k+1})$ as the mesh is refined, but the SDHM-C method presents results with a sub-optimal rate employing $k = l = 2$.

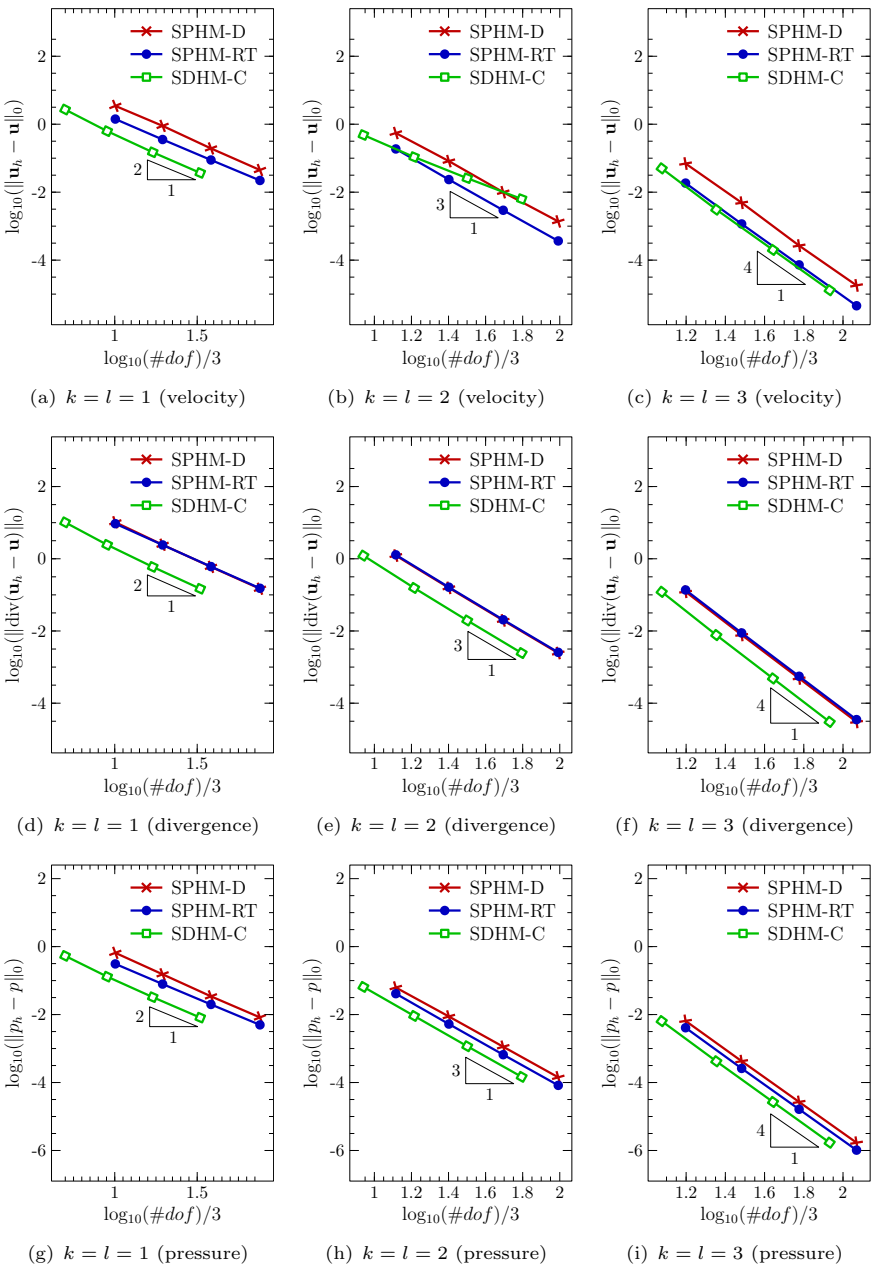

(a) $k = l = 1$ (velocity) (b) $k = l = 2$ (velocity) (c) $k = l = 3$ (velocity)

(d) $k = l = 1$ (divergence) (e) $k = l = 2$ (divergence) (f) $k = l = 3$ (divergence)

(g) $k = l = 1$ (pressure) (h) $k = l = 2$ (pressure) (i) $k = l = 3$ (pressure)

Figure 2. Numerical test case 2: h-convergence studies of the velocity (top), divergence (middle), and pressure (bottom) comparing SPHM-D, SPHM-RT, and SDHM-C in L^2-norm in terms of degrees of freedom.

6.2. Heterogeneous media

Here, we develop convergence studies considering heterogeneous media formed by variable, isotropic, or anisotropic hydraulic conductivity in two and three dimensions.

6.2.1. Numerical test Case 3

The next two-dimensional test case is inspired by the work of [20]. Supposing the domain $\Omega = [-2,2]^2$ formed by the union of Ω_1 and Ω_2, this test combines the solution (6.1) in $\Omega_1 = \Omega \setminus \Omega_2$ with the following pressure analytical solution in $\Omega_2 = [-1,1]^2$

$$p = \sin(\pi x)\sin(\pi y), \tag{6.3}$$

adopting $\mathbf{K} = \mathbf{I}$ in Ω_1 and in Ω_2 an anisotropic hydraulic conductivity tensor given by

$$\mathbf{K} = \begin{bmatrix} 2 & 1 \\ 1 & 2 \end{bmatrix}.$$

The results of this study are summarized in Figure 3. Compared with the results of the numerical test case presented in Section 6.1.1, it can be seen that the introduction of an anisotropic distribution of hydraulic conductivity in a domain region, despite generating velocity discontinuities, preserves the same convergence rates but with lower accuracy.

6.2.2. Numerical test Case 4

In the three-dimensional case, a low hydraulic conductivity block with $\mathbf{K} = \mathbf{I}$ is considered in $\Omega_1 = [-1/2, 1/2]^3$ and $\mathbf{K} = 100\mathbf{I}$ in $\Omega_2 = \Omega \setminus \Omega_1$, where $\Omega = [-1,1]^3$. For this test case, the pressure analytical solution is [1]

$$p = \exp\left(\left(x^2 - \frac{1}{4}\right)^2 \left(y^2 - \frac{1}{4}\right)^2 \left(z^2 - \frac{1}{4}\right)^2 - 1\right). \tag{6.4}$$

For this example, convergence rates and approximation errors are shown in Figure 4. It is possible to observe the same rates obtained in the test case considering the homogeneous medium depicted in Figure 2. However, for the velocity and pressure fields, the results in the heterogeneous medium show a decrease in the accuracy of the SDHM-C hybrid methodology concerning the other adopted hybrid approaches compared to the results in a homogeneous medium.

6.2.3. Numerical test Case 5

Let the square domain $\Omega = [-1,1]^2$, the next convergence test aims to study the effect of the following variable hydraulic conductivity adapted from [31]

$$\mathbf{K} = \begin{bmatrix} k_{xx} & 0 \\ 0 & k_{yy} \end{bmatrix}, \quad \text{with} \quad \begin{cases} k_{xx} = \exp(x+y), \\ k_{yy} = \exp(x-y) \end{cases}$$

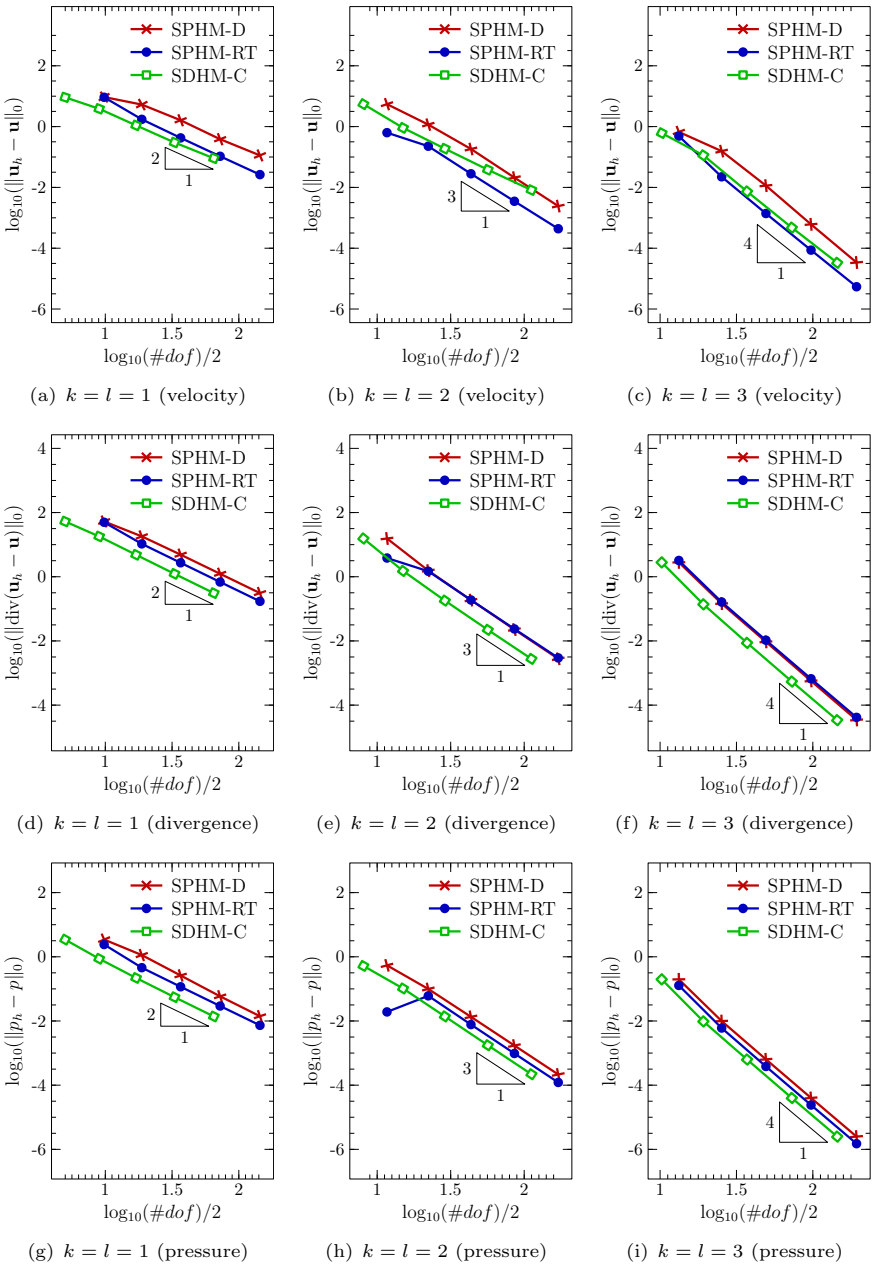

(a) $k = l = 1$ (velocity) (b) $k = l = 2$ (velocity) (c) $k = l = 3$ (velocity)

(d) $k = l = 1$ (divergence) (e) $k = l = 2$ (divergence) (f) $k = l = 3$ (divergence)

(g) $k = l = 1$ (pressure) (h) $k = l = 2$ (pressure) (i) $k = l = 3$ (pressure)

Figure 3. Numerical test case 3: h-convergence studies of the velocity (top), divergence (middle), and pressure (bottom) comparing SPHM-D, SPHM-RT, and SDHM-C in L^2-norm in terms of degrees of freedom.

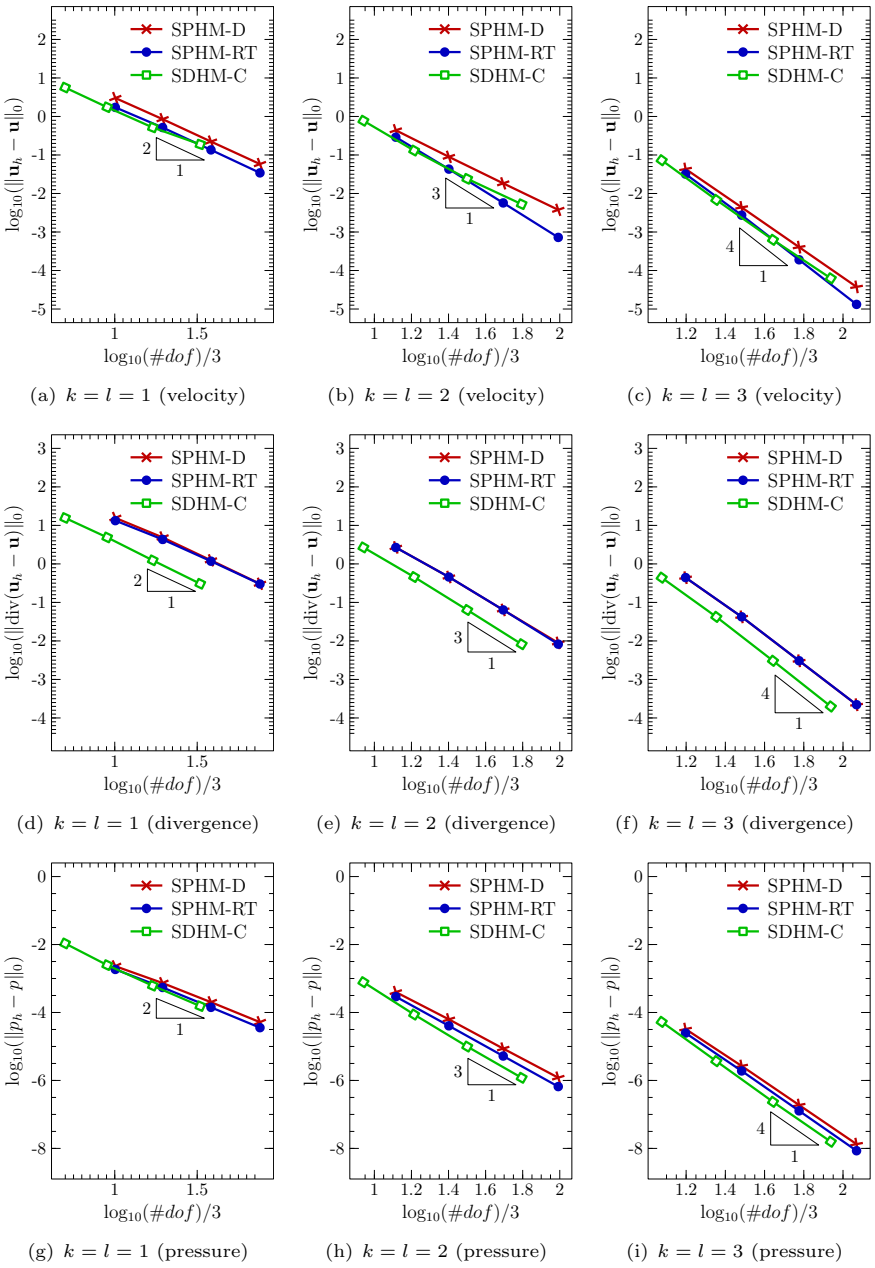

(a) $k = l = 1$ (velocity) (b) $k = l = 2$ (velocity) (c) $k = l = 3$ (velocity)

(d) $k = l = 1$ (divergence) (e) $k = l = 2$ (divergence) (f) $k = l = 3$ (divergence)

(g) $k = l = 1$ (pressure) (h) $k = l = 2$ (pressure) (i) $k = l = 3$ (pressure)

Figure 4. Numerical test case 4: h-convergence studies of the velocity (top), divergence (middle), and pressure (bottom) comparing SPHM-D, SPHM-RT, and SDHM-C in L^2-norm in terms of degrees of freedom.

whose analytical solution is given by

$$p = \sin(\pi x)\cos(\pi y). \tag{6.5}$$

The results presented in Figure 5 reproduce the convergence rates behavior of the previous studies, in particular, the numerical test case 3 (Section 6.2.1). Again, the optimal convergence rates are observed in all simulations for the pressure and divergence approximated by the hybrid methods and for the velocity field calculated by SPHM-D and SPHM-RT formulations. The velocity approximated by SDHM-C presents a sub-optimal convergence rate for polynomial order $k = l = 2$ and, in this case, is less accurate than SPHM-RT.

6.2.4. Numerical test Case 6

Similarly to the study developed in the previous subsection, but considering a three-dimensional domain $[-1, 1]^3$ and the following space-dependent hydraulic conductivity [31]

$$\mathbf{K} = \begin{bmatrix} k_{xx} & 0 & 0 \\ 0 & k_{yy} & 0 \\ 0 & 0 & k_{zz} \end{bmatrix}, \quad \text{with} \quad \begin{cases} k_{xx} = \exp(x+y), \\ k_{yy} = \exp(y+z), \\ k_{zz} = \exp(x+z) \end{cases}$$

whose analytical solution is given by

$$p = \sin(\pi x)\cos(\pi y)\sin(\pi z), \tag{6.6}$$

we present the convergence study in Figure 6. This study extends the problem simulated in Section 6.2.3 for the three-dimensional case. In this sense, we verify the similar results of the two-dimensional case, including a sub-optimal convergence rate demonstrated by the SDHM-C adopting $k = l = 2$.

6.3. p-convergence study

In this section, a p-convergence study of the previous numerical test cases is developed and presented in Figure 7. This study compares the hybrid methods SPHM-D, SPHM-RT, and SDHM-C for the velocity field regarding global degrees of freedom associated with Lagrange multipliers. For the simulations, we adopt uniform meshes with $2^4 \times 2^4$ quadrilateral elements and $2^3 \times 2^3 \times 2^3$ hexahedral elements considering polynomial approximations of the same order for velocity, pressure and multiplier with $k = l = 1, 2, 3, 4, 5, 6$ for two-dimensional cases and $k = l = 1, 2, 3, 4, 5$ for three-dimensional scenarios. In particular, for the SPHM-RT formulation, $k = l = 0$ is also simulated. The results show that by fixing the interpolation polynomial degree, the SPHM-RT method is more accurate than SPHM-D and SDHM-C for all polynomial orders simulated, differing only by the number of degrees of freedom due to the choice of the Lagrange multipliers. However, for the same number of degrees of freedom of the global problem, the method that uses continuous multipliers presents more accurate results.

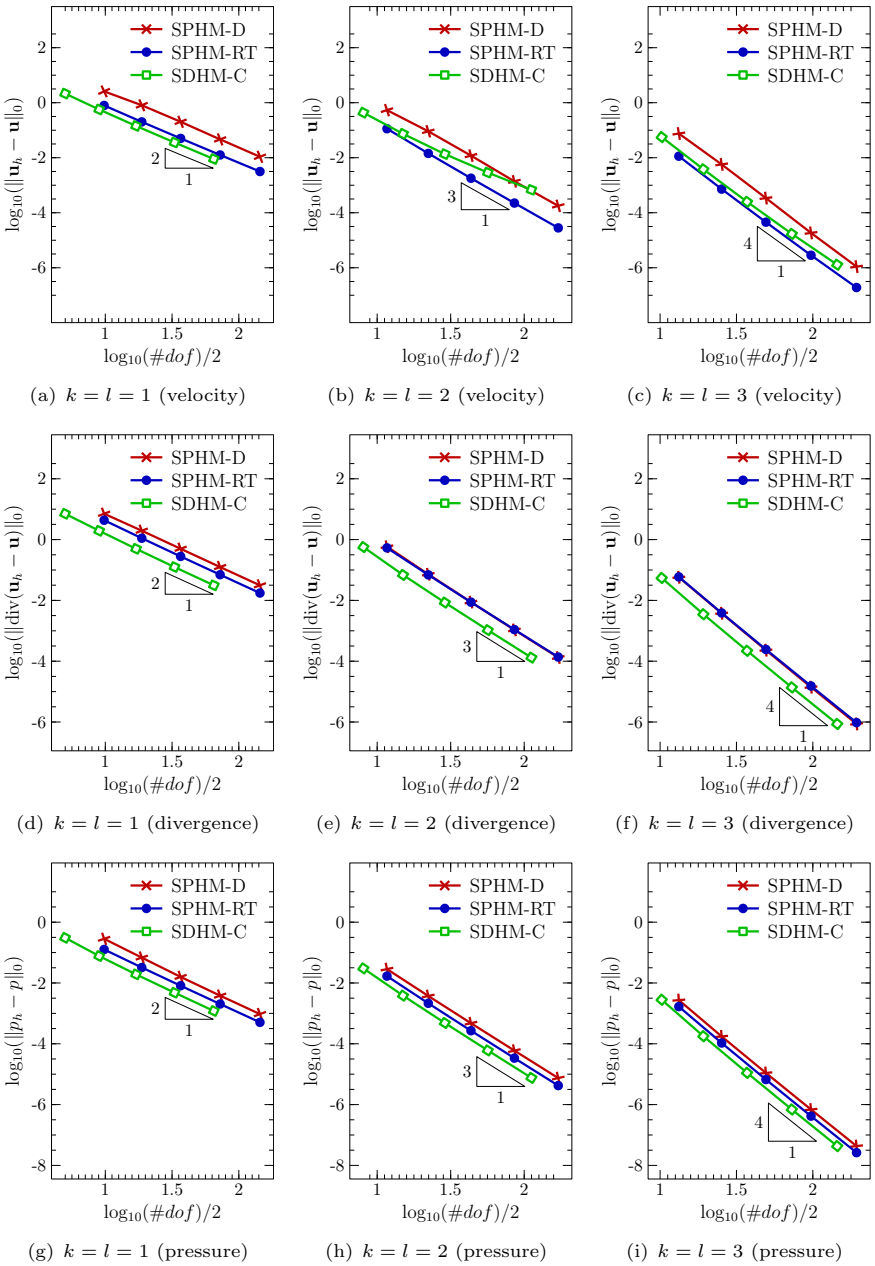

(a) $k = l = 1$ (velocity) (b) $k = l = 2$ (velocity) (c) $k = l = 3$ (velocity)

(d) $k = l = 1$ (divergence) (e) $k = l = 2$ (divergence) (f) $k = l = 3$ (divergence)

(g) $k = l = 1$ (pressure) (h) $k = l = 2$ (pressure) (i) $k = l = 3$ (pressure)

Figure 5. Numerical test case 5: h-convergence studies of the velocity (top), divergence (middle), and pressure (bottom) comparing SPHM-D, SPHM-RT, and SDHM-C in L^2-norm in terms of degrees of freedom.

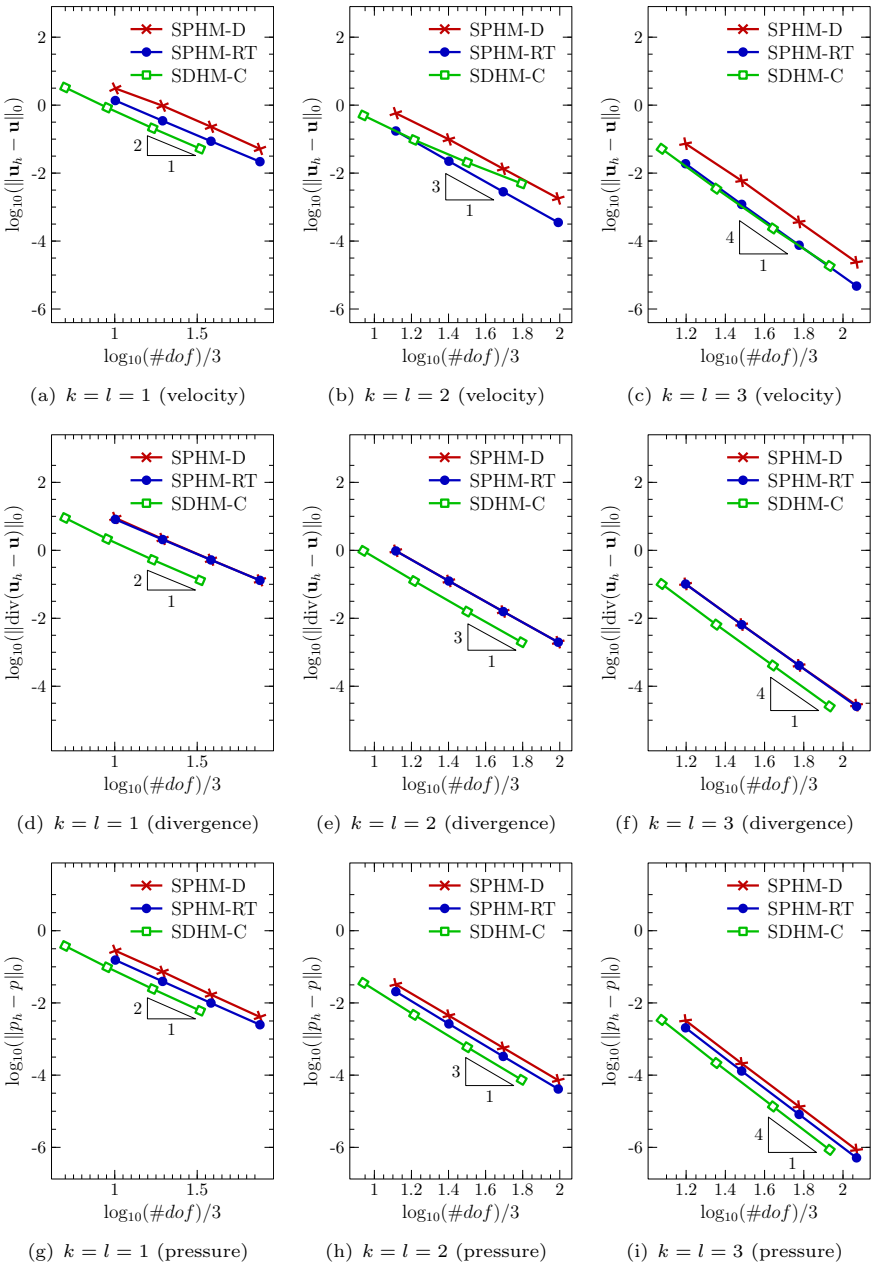

(a) $k = l = 1$ (velocity) (b) $k = l = 2$ (velocity) (c) $k = l = 3$ (velocity)

(d) $k = l = 1$ (divergence) (e) $k = l = 2$ (divergence) (f) $k = l = 3$ (divergence)

(g) $k = l = 1$ (pressure) (h) $k = l = 2$ (pressure) (i) $k = l = 3$ (pressure)

Figure 6. Numerical test case 6: h-convergence studies of the velocity (top), divergence (middle), and pressure (bottom) comparing SPHM-D, SPHM-RT, and SDHM-C in L^2-norm in terms of degrees of freedom ($\#dof$).

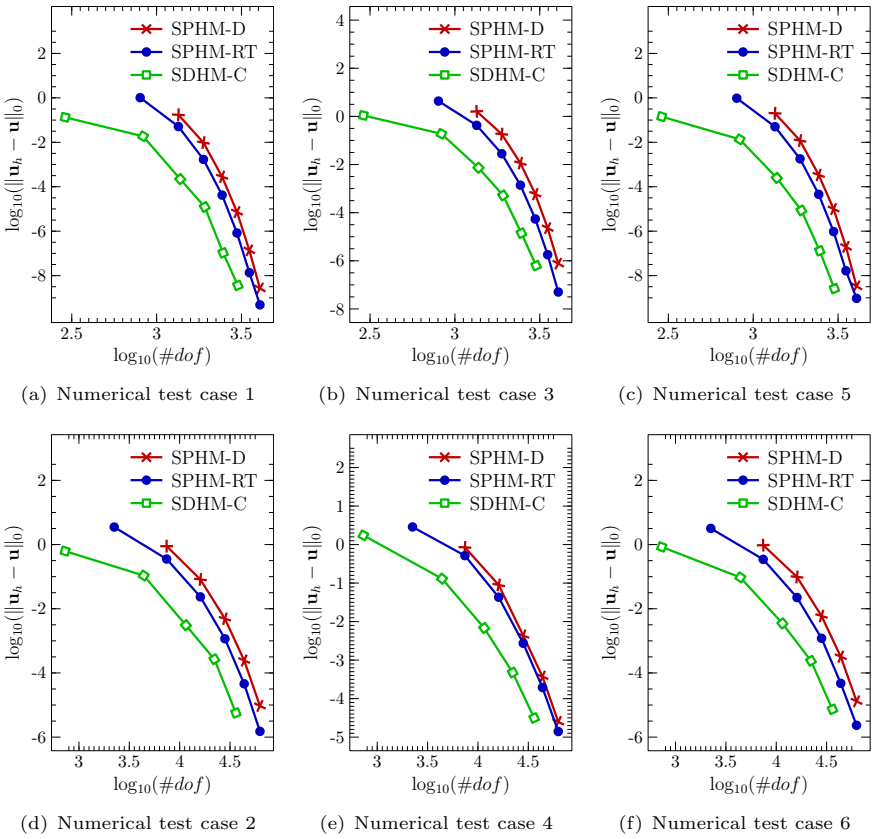

(a) Numerical test case 1 (b) Numerical test case 3 (c) Numerical test case 5

(d) Numerical test case 2 (e) Numerical test case 4 (f) Numerical test case 6

Figure 7. p-Convergence studies of the velocity field in two (top) and three (bottom) dimensions comparing SPHM-D, SPHM-RT, and SDHM-C in L^2-norm in terms of degrees of freedom.

6.4. Summary of convergence rates

Based on the numerical results of the h- and p-convergence, we summarize in Table 1 the convergence rates in $L2$ norm for velocity, divergence, and pressure obtained by SPHM-D, SPHM-RT, and SDHM-C. This table highlights the optimal convergence rates for all cases, except for the velocity field approximated by even polynomial orders using the SDHM-C method, which converges at a sub-optimal rate.

Table 1. Summary of convergence rates in the $L2$ norm of numerical test cases assuming polynomial orders $k = l > 0$ for SPHM-D and SDHM-C and $k = l \geq 0$ for SPHM-RT.

Error	SPHM-D	SPHM-RT	SDHM-C
$\|\mathbf{u} - \mathbf{u}_h\|_0$	$k+1$	$k+1$	$k+1$ (odd-order) k (even-order)
$\|\operatorname{div}(\mathbf{u} - \mathbf{u}_h)\|_0$	$k+1$	$k+1$	$k+1$
$\|p - p_h\|_0$	$k+1$	$k+1$	$k+1$

6.5. Local mass conservation

A local mass conservation study of the developed hybrid methods is presented in this section. This study aims to demonstrate the influence of parameter β_0 on the mass conservation of the SPHM-D and SPHM-RT methods in meshes composed of quadrilateral uniform elements. As a reference for this study, we compare the results obtained by the hybrid formulations with a classical formulation equipped by the conforming Raviart-Thomas spaces [29]. Thus, considering the same problem proposed in the Section 6.1 adopting meshes with 16×16 elements, we construct the results presented in Figure 8, where the β_0 parameter varies in the range between 10^{-2} and 10^{15}, and the local mass conservation (lmc) is calculated by the expression

$$lmc = \sqrt{\sum_{K \in \mathcal{T}_h} \sum_{e \in \partial K} \left(\int_e [\![\mathbf{u}_h]\!] \, ds \right)^2}.$$

Figure 8 shows that as the value β_0 is increased ($\beta_n \to \infty$), the hybrid methods tend to become locally conservative ($lmc \to 0$). This behavior occurs much earlier as the polynomial degree is increased. From a given β_0 value, the lmc reaches a plateau close to the result obtained with the classical Raviart-Thomas formulation. It is also possible to observe that the SPHM-RT method is more conservative than the SPHM-D for high values of stabilization parameter ($\beta_0 > 10^{10}$). In contrast, in most of the β_0 variation range, the SPHM-D method was more conservative. For the SDHM-C method, checking the local conservation property is unnecessary due to continuous interpolations for the Lagrange multiplier; in this case, lmc is unaffected by the β_0 parameter.

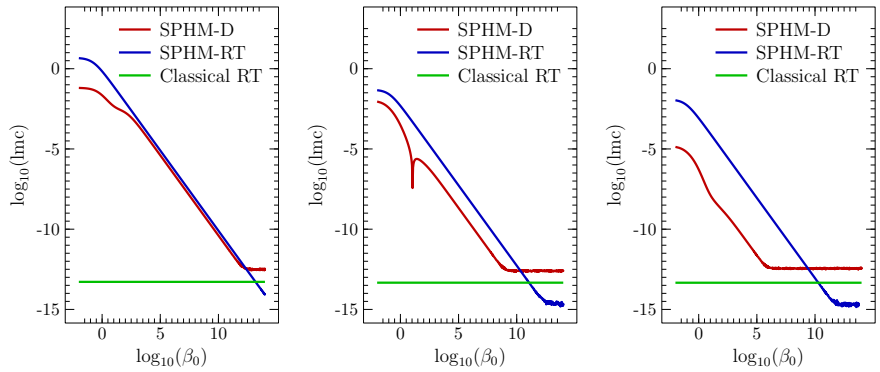

(a) Bilinear (b) Biquadratic (c) Bicubic

Figure 8. Influence of the stabilization parameter β_0 on the local mass conservation comparing SPHM-D and SPHM-RT formulations.

6.6. Computational efficiency

This section studies the computational efficiency of the SPHM and SDHM-C methods. In this context, we examine the number of iterations for convergence of the Conjugate Gradient method by comparing the Jacobi and SSOR preconditioners. Furthermore, we explore the computational costs associated with solving SPHM

and SDHM-C. For these studies, the three-dimensional problem related to numerical test case 6 was simulated for meshes of $2^4 \times 2^4 \times 2^4$, $2^5 \times 2^5 \times 2^5$ and $2^6 \times 2^6 \times 2^6$ elements and polynomial orders $k = l = 1, 2, 3$. It is important to highlight that we do not emphasize the approximation space of the SPHM method, as the results obtained with SPHM-D and SPHM-RT are similar.

Table 2 presents the number of iterations required to solve the linear system applying Jacobi and SSOR preconditioners for different mesh refinements and polynomial orders using a tolerance of 10^{-9}. In all results, the SSOR preconditioner consistently demonstrated faster convergence, requiring fewer iterations than the Jacobi preconditioner. Furthermore, as a result of employing discontinuous multipliers, the linear system produced by the SPHM method incorporates a greater number of variables than the one derived from the SDHM-C method, consequently requiring more iterations for convergence (see the values in parentheses in Figure 9).

Table 2. Number of iterations of the preconditioned conjugate gradient with the Jacobi and Symmetric Successive Over-Relaxation (SSOR) preconditioners using a tolerance of 10^{-9} to SPHM and SDHM-C methods for different mesh refinements and polynomial orders.

Mesh	Polynomial order	Jacobi		SSOR	
		SPHM	SDHM-C	SPHM	SDHM-C
$2^4 \times 2^4 \times 2^4$	$k = l = 1$	237	57	78	30
	$k = l = 2$	244	114	92	61
	$k = l = 3$	268	156	110	87
$2^5 \times 2^5 \times 2^5$	$k = l = 1$	404	120	140	57
$2^6 \times 2^6 \times 2^6$		766	248	271	111

A three-dimensional computational cost study of the SPHM and SDHM-C hybrid methods using the computer and the linear system solver described at the beginning of Section 6 is presented in Figure 9. This study is focused on the proportion of execution time between three steps of the resolution algorithm (see Section 5), which are Assembly, Linear system, and Post-processing. The Assembly considers the local problems assembly, static condensation, and global problem assembly. The Linear system is related to the solution of the global matrix, in which entries are associated with the Lagrange multipliers' degrees of freedom. Post-processing accounts for the cost to find, given the multiplier approximation, the solution of the interest variables in each element.

As expected, the results show that using continuous multipliers (SDHM-C) compared to discontinuous multipliers (SPHM) presents a reduction in computational cost for all simulated cases, and this cost reduction is proportionally preserved when we increase the polynomial order (see Fig. 9(a)). Moreover, when we increase the polynomial order, we can also observe that the cost to solve the linear system is negligible compared to the steps of static condensation combined with global problem assembly. On the other hand, when we increase the mesh refinement (see Fig. 9(b)) using discontinuous multipliers, we see that the computational cost of solving the linear system becomes higher than the other steps of the resolution algorithm. This is because the mesh refinement generates more element faces, increasing the global problem (see the degrees of freedom in parentheses in Fig. 9(b)). However,

continuous multipliers preserve the low cost of solving the linear system, and, in this case, the Assembly stage predominantly dominates the computational cost as illustrated in Figure 9(b)). The post-processing step presents the lowest computational cost in all cases studied due to the storage of $\mathbf{A}_K^{-1}$, which allows a direct substitution of the Lagrange multiplier solution in 5.7 to find velocity and pressure.

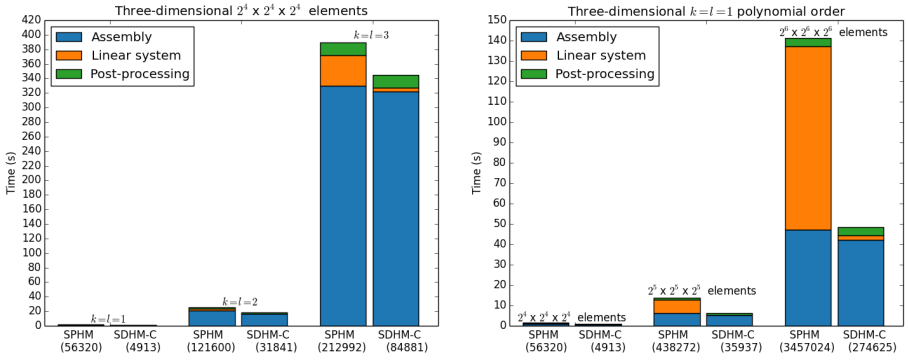

(a) polynomial order increase (b) mesh refinement increase

Figure 9. Three-dimensional computational cost of assembly, linear system solver, and post-processing comparing SPHM and SDHM-C formulations increasing the polynomial order and mesh refinement.

7. Discussions

Convergence studies for the hybrid mixed method employing continuous multipliers demonstrated optimal convergence rates for the primal scalar variable in all simulated scenarios. Although this approach does not preserve local mass conservation, its computational cost is considerably reduced compared to methodologies that adopt discontinuous multipliers, as illustrated in Section 6.6. In this sense, this methodology favors applications that show similarities with the model problem studied in this work but have the scalar variable as the main one of the model [21, 23, 27, 30]. Among the possible applications for this methodology, we highlight the Helmholtz problem, the transport problem, the Cahn-Hilliard problem, and the cardiac monodomain problem, among others.

A hybrid method for the mixed Darcy problem employing continuous interpolations for the Lagrange multiplier was proposed and analyzed in [16]. The stability of this formulation is enforced by penalty terms defined on the interface of the elements (similar to the term multiplied by β in this work). It presents optimal convergence rates for pressure and sub-optimal for the velocity field. The SDHM-C formulation proposed and analyzed in this work demonstrates an advance in this direction. Since including least-squares terms provides optimal rates for the velocity field when applying odd-order polynomial approximations.

The proposed SPHM formulation, due to the choice of the multiplier associated with the normal velocity component, can be used to simulate coupled problems where the interface conditions are compatible with this choice for the multiplier. In this context, numerical approaches can be proposed using hybrid methods that couple the SPHM method, using standard polynomial basis or Raviart-Thomas

spaces, with other methodologies present in the literature for problems such as Stokes/Darcy, Navier-Stokes/Darcy, and Helmholtz/elastic wave.

Although it was not the subject of this work, due to the use of broken spaces, these methodologies are naturally indicated for the benefit of parallelism approaches and adaptivity schemes for the simulation of large problems that demand high numerical accuracy. Thus, using computational parallelism and mesh or polynomial adaptivity could be easily handled by hybrid methods [31]. The application of parallelism techniques, mainly using high-order polynomial interpolations, can overcome the most computationally expensive step of the SDHM-C method. In this case, as demonstrated in the computational efficiency results, assembling the linear system associated with the global problem using high-order polynomials can dominate the computational cost, as seen in Figure 9(a). In this context, the use of parallelization strategies in the assembly stage can substantially reduce the problem's computational cost.

Regarding the variation of the β penalty parameter, it is important to emphasize that the increase of β_n to achieve local conservation can affect the conditionality of the matrix associated with the linear system generated by the SPHM method. In practice, what is noticed in the results presented in Section 6.5 is that there is an increase in the number of iterations of the linear system solver, whereas, for the bilinear case, it can be observed that the number of iterations from the lowest to the highest β_0, practically doubles. For the biquadratic case, they quadruple, and so on. On the other hand, the SDHM method remains well-conditioned since taking $\beta_p = 0$ does not affect the matrix stability due to the least-squares terms.

8. Conclusion and remarks

Stabilized Primal and Dual hybrid formulations were presented and analyzed in this work, where the principal difference between the proposed methods is the choice of the Lagrange multipliers. The stability of these methods was improved by adding least-square residuals of the governing equations, besides the classical stabilizations associated with the Lagrange multipliers on the edge/face of the elements. The analysis of the proposed methods started from the connection of these methods with the same discontinuous Galerkin formulation. Thus, the same mathematical tools proved both methods' consistency, stability, continuity, and error estimates.

As summarized in Table 1, the convergence results demonstrated optimal convergence rates for the pressure field and the divergence even in heterogeneous media for all studied cases. For the velocity field, optimal convergence rates are verified using discontinuous multipliers. Conversely, the convergence order is degraded for continuous multipliers when even-order polynomials are adopted. Regarding the number of degrees of freedom, continuous interpolations for the Lagrange multiplier showed more accurate results than discontinuous multipliers, especially for pressure, divergence, and using bilinear approximations for the velocity field.

Numerical tests have ensured that the methods that employ discontinuous multipliers become locally conservative for specific limits of the edge/face stabilization parameter. Moreover, a study of the computational cost in three dimensions showed that assembling the linear system is the most expensive step in solving the methods using high-order polynomials. However, by fixing the polynomial order and refining the mesh, the computational cost to solve the linear system increases considerably, exceeding the assembly cost. We also showed that, in general, the iterative CG

method with the SSOR preconditioner required only half the iterations for convergence of the linear system compared to the Jacobi preconditioner. Finally, as discussed, the proposed methods can also be extended or adapted to other physical applications, aiming to reduce the computational cost through continuous multipliers or expand the possibilities of combining with other numerical methodologies to treat coupled problems.

References

[1] P. F. Antonietti and L. Heltai, *Numerical validation of a class of mixed discontinuous Galerkin methods for Darcy flow*, Computer Methods in Applied Mechanics and Engineering, 2007, 196(45), 4505–4520.

[2] T. Arbogast and M. R. Correa, *Two families of H(div) mixed finite elements on quadrilaterals of minimal dimension*, SIAM Journal on Numerical Analysis, 2016, 54(6), 3332–3356.

[3] D. Arndt, W. Bangerth, M. Feder, et al., *The `deal.II` library, version 9.4*, Journal of Numerical Mathematics, 2022, 30(3), 231–246.

[4] D. Arndt, W. Bangerth, M. Feder, et al., *An interior penalty finite element method with discontinuous elements*, SIAM Journal on Numerical Analysis, 1982, 19(4), 742–760.

[5] D. N. Arnold, D. Boffi and R. S. Falk, *Quadrilateral H(div) finite elements*, SIAM Journal on Numerical Analysis, 2005, 42(6), 2429–2451.

[6] D. N. Arnold and F. Brezzi, *Mixed and nonconforming finite element methods: Implementation, postprocessing and error estimates*, ESAIM: M2AN, 1985, 19(1), 7–32.

[7] D. N. Arnold, F. Brezzi, B. Cockburn and L. D. Marini, *Unified analysis of discontinuous Galerkin methods for elliptic problems*, SIAM Journal on Numerical Analysis, 2002, 39(5), 1749–1779.

[8] N. C. Arruda, A. F. Loula and R. C. Almeida, *Locally discontinuous but globally continuous Galerkin methods for elliptic problems*, Computer Methods in Applied Mechanics and Engineering, 2013, 255, 104–120.

[9] I. Babuška, *Error-bounds for finite element method*, Numerische Mathematik, 1971, 16(4), 322–333.

[10] G. R. Barrenechea, L. P. Franca and F. Valentin, *A Petrov–Galerkin enriched method: A mass conservative finite element method for the Darcy equation*, Computer Methods in Applied Mechanics and Engineering, 2007, 196(21), 2449–2464.

[11] D. Boffi, F. Brezzi and M. Fortin, *Mixed Finite Element Methods and Applications*, Springer Berlin, Heidelberg, 2013.

[12] F. Brezzi, *On the existence, uniqueness and approximation of saddle-point problems arising from Lagrange multipliers*, Revue Française d'Automatique Informatique et Recherche Opérationnelle, Séries Rouge, 1974, 8(R–2), 129–151.

[13] F. Brezzi, J. Douglas and L. Marini, *Two families of mixed finite elements for second order elliptic problems*, Numerische Mathematik, 1985, 47, 217–235.

[14] F. Brezzi and M. Fortin, *A minimal stabilisation procedure for mixed finite element methods*, Numerische Mathematik, 2001, 89(3), 457–491.

[15] F. Brezzi, T. J. R. Hughes, L. D. Marini and A. Masud, *Mixed discontinuous Galerkin methods for Darcy flow*, Journal of Scientific Computing, 2005, 22(1), 119–145.

[16] B. Cockburn, J. Gopalakrishnan and R. Lazarov, *Unified hybridization of discontinuous Galerkin, mixed and continuous Galerkin methods for second order elliptic problems*, SIAM Journal on Numerical Analysis, 2009, 47(2), 1319–1365.

[17] B. Cockburn, J. Guzmán, S.-C. Soon and H. K. Stolarski, *An analysis of the embedded discontinuous Galerkin method for second-order elliptic problems*, SIAM Journal on Numerical Analysis, 2009, 47(4), 2686–2707.

[18] B. Cockburn and W. Zhang, *A posteriori error estimates for HDG methods*, Journal of Scientific Computing, 2012, 51(3), 582–607.

[19] M. Correa and A. Loula, *Unconditionally stable mixed finite element methods for Darcy flow*, Computer Methods in Applied Mechanics and Engineering, 2008, 197(17–18), 1525–1540.

[20] P. Crumpton, G. Shaw and A. Ware, *Discretisation and multigrid solution of elliptic equations with mixed derivative terms and strongly discontinuous coefficients*, Journal of Computational Physics, 1995, 116(2), 343–358.

[21] R. Griesmaier and P. Monk, *Error analysis for a hybridizable discontinuous Galerkin method for the Helmholtz equation*, Journal of Scientific Computing, 2011, 49(3), 291–310.

[22] T. J. Hughes, A. Masud and J. Wan, *A stabilized mixed discontinuous Galerkin method for Darcy flow*, Computer Methods in Applied Mechanics and Engineering, 2006, 195(25), 3347–3381.

[23] I. Igreja and G. de Miranda, *Hybrid mixed methods applied to miscible displacements with adverse mobility ratio*, in Computational Science – ICCS 2020 (Edited by V. V. Krzhizhanovskaya, G. Závodszky, M. H. Lees, et al.), Springer International Publishing, 2020, 257–268.

[24] I. Igreja and A. F. D. Loula, *Stabilized velocity and pressure mixed hybrid DGFEM for the Stokes problem*, International Journal for Numerical Methods in Engineering, 2017, 112(7), 603–628.

[25] I. Igreja and A. F. D. Loula, *A stabilized hybrid mixed DGFEM naturally coupling Stokes–Darcy flows*, Computer Methods in Applied Mechanics and Engineering, 2018, 339, 739–768.

[26] A. Masud and T. J. Hughes, *A stabilized mixed finite element method for Darcy flow*, Computer Methods in Applied Mechanics and Engineering, 2002, 191(39), 4341–4370.

[27] E. Y. Medina, E. M. Toledo, I. Igreja and B. M. Rocha, *A stabilized hybrid discontinuous Galerkin method for the Cahn–Hilliard equation*, Journal of Computational and Applied Mathematics, 2022, 406, 114025.

[28] Y. R. Núñez, C. O. Faria, A. F. D. Loula and S. M. C. Malta, *Um método híbrido de elementos finitos aplicado a deslocamentos miscíveis em meios porosos heterogêneos*, Revista Internacional de Métodos Numéricos para Cálculo y Diseño en Ingeniería, 2017, 33(1), 45–51.

[29] P. A. Raviart and J. M. Thomas, *A mixed finite element method for second order elliptic problems*, Mathematical Aspects of the FEM. Lecture Notes in Mathematics, 1977, 606, 292–315.

[30] B. M. Rocha, R. W. dos Santos, I. Igreja and A. F. D. Loula, *Stabilized hybrid discontinuous Galerkin finite element method for the cardiac monodomain equation*, International Journal for Numerical Methods in Biomedical Engineering, 2020, 36(7), e3341.

[31] A. Samii, C. Michoski and C. Dawson, *A parallel and adaptive hybridized discontinuous Galerkin method for anisotropic nonhomogeneous diffusion*, Computer Methods in Applied Mechanics and Engineering, 2016, 304, 118–139.